Supplement

Rewiring of genetic networks in response to modification of genetic background

Djordje Bajić, Clara Moreno and Juan F. Poyatos

Logic of Genomic Systems Laboratory, CNB-CSIC, Madrid, Spain

Flux change associated to metabolite production correlates with genetic rewiring in catabolic but not in biosynthetic metabolites

We summed the metabolic fluxes contributing to the production of a particular metabolite (m) in WT conditions (Σ^m_{wt}), and in each of the backgrounds (bg$i$) defined by deletions of single genes ($\Sigma^m_{\text{bg}i}$). We divided both measures (each one normalized by their corresponding flux of the biomass reaction, that we denote Ξ^m_{wt} and $\Xi^m_{\text{bg}i}$) to compute the fold-change of metabolite m production in all backgrounds (i.e., $\Xi^m_{\text{bg}i}/\Xi^m_{\text{wt}}$). Fold-change in most metabolites significantly correlates with genetic rewiring (table S1, this is consistent with the association between genetic rewiring and metabolic readjustment; see also main text).

Notably, correlations are stronger for redox equivalents and currency metabolites (nadh, nadph, h, phosphate, atp), the serine → glycine → formate pathway intermediates (e.g., thf, mlthf, for, phosphoserine, serine, glycine), oxidative phosphorylation metabolites (e.g., quinones), glycolytic intermediates (e.g., glucose, glucose-6-phosphate, f6p, g3p, pyruvate) and TCA cycle intermediates (alpha ketoglutarate, isocitrate, oxaloacetate). Conversely, most intermediates from diverse biosynthetic pathways either correlate more weakly or do not correlate at all with genetic rewiring.

Catabolism in the *Sacharomyces cerevisiae* `iND750` model

Catabolic action consists of the breakdown of nutrients into energy (usually in the form of ATP), reduced equivalents (e.g., NADH, NADPH), and smaller components to be involved in

biosynthetic reactions (precursors). All of this can be produced in the oxidative pathway after initial glucose uptake, through glycolysis and citric acid cycle (or tricarboxilic acid cycle, TCA). In addition, the most efficient ATP production pathway in aerobic conditions is oxidative phosphorylation that is able to couple the oxidation of reduced equivalents (produced in glycolysis and TCA cycle) to ATP synthesis. Thus, a considerable proportion of the flux through both glycolysis and TCA cycle is devoted to the supply of reduced equivalents to oxidative phosphorylation.

Beyond these "canonical" catabolic pathways, the `iND750` model also predicts artifactually the production of an important fraction of ATP. Specifically, part of the glycolytic 3-phosphoglycerate is diverted towards serine and then glycine that later becomes fermented to CO2 by the glycine cleavage system. This cycle also produces formate that is then oxidized to CO2 while at the same time reducing quinone, thereby also feeding oxidative phosphorylation. The model predicts this pathway as one of the main catabolic ones. For instance, this pathway takes over ATP production (accounting for about 60% of the total; see table S2) when oxidative phosphorylation is compromised (e.g., in the ΔCOX1 background). Note as well that the pathway includes genes from several annotation groups that would not be expected to contribute to glucose catabolism, such as the glycine/serine (e.g., SER1, SER2), or the folate group (e.g., GCV3). Certainly, this form of "glycine fermentation" is artifactual in yeast, and we found only one reference to a similar metabolic process occuring in *Clostridium purinolyticum* [1]. This catabolic role determines the rewiring and stability properties of the associated genes, and indeed they act in a similar way to the rest of "canonical" members of catabolic pathways (e.g., there is an abundance of genetic interactions between SER1 or SER2 with glycolytic, TCA cycle or oxidative phosphorylation genes; see Fig. 3, main text).

Other genes that belong to biosynthetic annotation groups also displayed epistatic interactions characteristic of catabolism (i.e., weak interactions with other genes of the catabolic core), such as AAT1, ALD6, or ALT2 (all associated to the Tyr, Trp and Phe group). This is due to their role in inter-conversions important for catabolic balances, such as α-ketoglutarate $\rightleftharpoons$ ox-

aloacetate, acetate $\rightleftharpoons$ acetaldehide and α-ketoglutarate $\rightleftharpoons$ pyruvate, respectively. On the other hand, they also exhibit several synthetic lethal interactions that are linked to their biosynthetic roles (more details below).

Genetic interaction stability as a function of sign, strength and functional association

In Fig. S1, we show the difference in interaction stability for different types of interactions. Interactions between genes in the same metabolic annotation module are more stable than those between different annotation groups; strong interactions are more stable than weak, and negative interactions are more stable than positive. To eliminate possible confounding effects between these factors, we performed separated Wilcoxon tests controlling for each of these factors, generally confirming the independent influence of all three on stability (table S4).

Case study: Metabolic reorganization and genetic rewiring in the ΔMIR1 genetic background

In order to better understand the metabolic underpinnings of genetic rewiring, we analyzed in detail the changes occuring in the `MIR1` background, the mitochondrial phosphate carrier needed to provide phosphate for ATP synthesis through phosphorylative oxidation. This gene represents a typical example of genetic hub, with 31 epistatic interactions (24 of these being weak) that encompas 16 different metabolic modules (many of them are clearly biosynthetic, e.g., Arg/Pro or Thr/Lys).

In Fig. S3, we schematically depict some of the relevant metabolic changes that occur after deletion of this gene. The impairment in phosphate import to mitochondria caused by the deletion is "solved" in first instance by the antiport of phosphate with malate by the gene `DIC1`. Malate is then transformed to oxaloacetate in order to be reimported to mitochondria. This process results in a net extrusion of redox equivalents to cytosol that works as a kind of "redox shuttle". Ultimately, many metabolic pathways readjust to buffer the generated imbalance

(including some biosynthetic ones that conceal redox-balancing possibilities). Specific examples include:

- Proline starts being synthesized from orotate in the cytosol to be then imported to mitochondria, where it becomes tranformed again into orotate through several steps. The entire process transports redox equivalents from cytosol (NADPH) to mitochondria (NADH) and converts an additional molecule of mitochondrial NADPH into NADH.
- The glycine cleavage system (artifactually) stops synthesizing ATP and redox equivalents, avoiding further release of NADH and NADPH to the cytosol. As a consequence, respiratory activity increases as compared to the WT.
- First steps of lipid synthesis from DHAP switch to an alternative pathway using NADH instead of NADPH.
- Further reorganizations (Fig. S3).

How are all these changes reflected on the genetic landscape? Firstly, activated compensatory mechanisms (e.g., mitochondrial malate synthesis and its cytosolic conversion to oxalacetate) start interacting positively with those genes experiencing the buffering changes (i.e., genes in the oxidative phosphorylation apparatus) but also among them, as part of the new optimal solution (Fig. S4). Second, since different compensatory mechanisms often contribute to similar functions (e.g., importing redox power to mitochondria) they can in turn interact negatively interacting among them (e.g., PUT1 and ALD6). Finally, newly revealed negative interactions can reflect as well third-instance alternatives able to compensate for the loss of some genes in the new solution. These types of genetic rewiring are summarized in Fig. S5.

metabolite	Spearman ρ	metabolite	Spearman ρ	metabolite	Spearman ρ
h[c]	0.89†	13dpg[c]	0.76‡	paps[c]	0.15
h[m]	0.88†	3pg[c]	0.76‡	so3[c]	0.15
nad[m]	0.86†	ficytc[m]	0.76‡	so4[c]	0.15
nadh[m]	0.86†	focytc[m]	0.76‡	so4[e]	0.15
nad[c]	0.85†	o2[m]	0.76‡	trdox[c]	0.15
nadh[c]	0.85†	o2[c]	0.76‡	trdrd[c]	0.15
nadp[c]	0.83†	o2[e]	0.76‡	ppi[c]	0.15
nadph[c]	0.83†	dhap[c]	0.76‡	2cpr5p[c]	0.13
pi[c]	0.82†	fdp[c]	0.76‡	3ig3p[c]	0.13
thf[c]	0.81†	glu_L[c]	0.76‡	anth[c]	0.13
co2[m]	0.81†	h2o[e]	0.76‡	pran[c]	0.13
mlthf[c]	0.8†	g6p[c]	0.76‡	utp[c]	-0.1
gly[m]	0.79†	glc_D[e]	0.76‡	25aics[c]	0.1
thf[m]	0.79†	f6p[c]	0.76‡	34hpp[c]	0.1
mlthf[m]	0.79†	pyr[m]	0.64‡	5aizc[c]	0.1
h2o[c]	0.79†	icit[m]	0.62‡	aicar[c]	0.1
pi[m]	0.79‡	1agly3p_SC[c]	0.62*	air[c]	0.1
for[c]	0.79‡	oaa[c]	0.6*	dcamp[c]	0.1
3php[c]	0.79‡	akg[m]	0.6*	fgam[c]	0.1
pser_L[c]	0.79‡	acald[c]	0.57*	fpram[c]	0.1
ser_L[c]	0.79‡	2pg[c]	0.57*	fprica[c]	0.1
10fthf[c]	0.78‡	pep[c]	0.57*	fum[c]	0.1
methf[c]	0.78‡	cit[m]	0.56*	gar[c]	0.1
nh4[m]	0.78‡	nadp[m]	0.56*	gln_L[c]	0.1
co2[c]	0.78‡	ac[c]	0.55*	imp[c]	0.1
nh4[c]	0.78‡	accoa[c]	0.55*	pi[e]	0.1
atp[m]	0.77‡	coa[c]	0.55*	pram[c]	0.1
akg[c]	0.77‡	pyr[c]	0.54*	ctp[c]	-0.09
gly[c]	0.77‡	coa[m]	0.54*	dudp[c]	-0.09
h2o[m]	0.77‡	accoa[m]	0.54*	dump[c]	-0.09
glc_D[c]	0.76‡	asp_L[c]	0.54*	prpp[c]	0.08
atp[c]	0.76‡	oaa[m]	0.53*	gdp[c]	-0.04
adp[c]	0.76‡	nadph[m]	0.51*	gtp[c]	-0.04
adp[m]	0.76‡	mal_L[c]	0.46*	g1p[c]	0.04
q6[m]	0.76‡	hco3[c]	0.43*	ps_SC[m]	0.04
q6h2[m]	0.76‡	asp_L[m]	0.43*	tre6p[c]	0.04
co2[e]	0.76‡	aps[c]	0.15	udp[c]	0.04
g3p[c]	0.76‡	pap[c]	0.15	udpg[c]	0.04

Table S1. Fold-change of metabolic production significantly correlates with rewiring, a signal that appears particularly strong in catabolic metabolites ($^{\dagger}P < 10^{-20}$, $^{\ddagger}P < 10^{-10}$, $^{\star}P < 0.01$). Metabolites are colored according to broad functional context where they appear. Red–catabolism; blue–biosynthesis; violet–currency metabolites and related molecules (e.g., H^{+} or phosphate); yellow–metabolites belonging to artifactually catabolic pathways (see below), gray–other types fo metabolites (such as water, inorganic nutrients, etc.).

		ATP synthesis mechanisms		
		ATP synthase	FTHFL	PGK + PK
Background	WT	100 (60%)	26 (16%)	37 (23%)
	ΔCOX1	0	54 (60%)	36 (40%)

Table S2. ATP production ($mmol\ grDW^{-1}\ h^{-1}$) by different mechanisms in WT and in ΔCOX1 background (percentage of the total ATP produced in the cell in each case in parenthesis). FTHFL: formate tetrahydrofolate ligase, PGK: phosphoglycerate kinase, PK: pyruvate kinase. See second section Supplement for details.

G1	G2	iWT	G1 annotation	G2 annotation
ACH1	ACS2	-1	Pyr	Pyr
ARO4	ARO3	-1	TyrTrpPhe	TyrTrpPhe
CTP1	SER2	-1	MitTrnsp	GlySer
CTP1	AAT1	-1	MitTrnsp	AlaAsp,ArgPro,TyrTrpPhe
CTP1	SER1	-1	MitTrnsp	GlySer,Pdx
APA1	MET3	-1	Cys,PurPyr	Cys
PMP1	MET22	-1	ExtclTrnsp	Cys
THR4	GLY1	-1	ThrLys	ThrLys
TPI1	PFK1	-1	Glycls	Glycls
TPI1	FBA1	-1	Glycls	Glycls
ALT2	SER2	-1	AlaAsp	GlySer
ALT2	BNA2	-1	AlaAsp	TyrTrpPhe
ALT2	BNA5	-1	AlaAsp	TyrTrpPhe
ALT2	SER1	-1	AlaAsp	GlySer,Pdx
HOM2	GLY1	-1	AlaAsp	ThrLys
HOM2	IRC7	-1	AlaAsp	Met
HOM2	YML082W	-1	AlaAsp	Met
PRO1	CAR2	-1	ArgPro	ArgPro
GLY1	HOM3	-1	ThrLys	AlaAsp
GLY1	THR1	-1	ThrLys	GlySer
GLY1	HOM6	-1	ThrLys	GlySer
HOM3	IRC7	-1	AlaAsp	Met
HOM3	YML082W	-1	AlaAsp	Met
ICL1	SER2	-1	Anapl.	GlySer
ICL1	SER1	-1	Anapl.	GlySer,Pdx
AGX1	SER2	-1	GlySer	GlySer
AGX1	SER1	-1	GlySer	GlySer,Pdx
IRC7	HOM6	-1	Met	GlySer
IRC7	MET17	-1	Met	Met
IRC7	MET2	-1	Met	Met
PSD2	PSD1	-1	Plip	Plip
ACO2	ACO1	-1	TCAcycle	TCAcycle
HOM6	YML082W	-1	GlySer	Met
AAT1	AAT2	-1	AlaAsp,ArgPro,TyrTrpPhe	AlaAsp,ArgPro,TyrTrpPhe
AAT1	IDP2	-1	AlaAsp,ArgPro,TyrTrpPhe	TCAcycle
CAR2	PRO2	-1	ArgPro	ArgPro
YML082W	MET2	-1	Met	Met
TSL1	TPS3	-1	AltCS	AltCS
ADH3	ALD6	-1	Glip	TyrTrpPhe
LEU4	LEU9	-1	ValLeuIle	ValLeuIle
PSD1	ATH1	-1	Plip	AltCS
ALD4	ALD6	-1	OAA,TyrTrpPhe	TyrTrpPhe

Table S3. Distribution of genetic interactions in catabolic modules.

G1	G2	iWT	G1 annotation	G2 annotation
COX1	GCV3	-0.5	OxPhos	Folate,GlySer
COX1	TPI1	-0.5	OxPhos	Glycls
COX1	LPD1	-0.5	OxPhos	TCAcycle,GlySer,Glycls
COX1	CTT1	-0.5	OxPhos	TyrTrpPhe
COX1	SER2	-0.5	OxPhos	GlySer
COX1	PFK1	-0.5	OxPhos	Glycls
COX1	MAE1	-0.5	OxPhos	Anapl.
COX1	FBA1	-0.5	OxPhos	Glycls
COX1	SER1	-0.5	OxPhos	GlySer,Pdx
ATP8	TPI1	-0.5	OxPhos	Glycls
ATP8	LPD1	-0.5	OxPhos	TCAcycle,GlySer,Glycls
ATP8	CTT1	-0.5	OxPhos	TyrTrpPhe
ATP8	PFK1	-0.5	OxPhos	Glycls
ATP8	FBA1	-0.5	OxPhos	Glycls
COB	GCV3	-0.5	OxPhos	Folate,GlySer
COB	TPI1	-0.5	OxPhos	Glycls
COB	LPD1	-0.5	OxPhos	TCAcycle,GlySer,Glycls
COB	CTT1	-0.5	OxPhos	TyrTrpPhe
COB	SER2	-0.5	OxPhos	GlySer
COB	PFK1	-0.5	OxPhos	Glycls
COB	MAE1	-0.5	OxPhos	Anapl.
COB	FBA1	-0.5	OxPhos	Glycls
COB	SER1	-0.5	OxPhos	GlySer,Pdx
GCV3	KGD2	-0.5	Folate,GlySer	TCAcycle,Glycls
GCV3	SER2	-0.5	Folate,GlySer	GlySer
GCV3	LSC2	-0.5	Folate,GlySer	TCAcycle
GCV3	SDH2	-0.5	Folate,GlySer	TCAcycle,OxPhos
GCV3	IDH1	-0.5	Folate,GlySer	TCAcycle
GCV3	SER1	-0.5	Folate,GlySer	GlySer,Pdx
GCV3	FUM1	-0.5	Folate,GlySer	OxPhos
YAT1	LPD1	-0.5	AlaAsp	TCAcycle,GlySer,Glycls
YAT1	MIR1	-0.5	AlaAsp	MitTrnsp
ACH1	PDB1	-0.5	Pyr	Folate,Glycls
ACH1	PMP1	-0.5	Pyr	ExtclTrnsp
ACH1	LPD1	-0.5	Pyr	TCAcycle,GlySer,Glycls
ACH1	MIR1	-0.5	Pyr	MitTrnsp
ACH1	LAT1	-0.5	Pyr	Glycls
UGA2	LPD1	-0.5	Glu	TCAcycle,GlySer,Glycls
PGI1	TPI1	-0.5	Glycls	Glycls
PGI1	PFK1	-0.5	Glycls	Glycls
PGI1	GRE3	-0.5	Glycls	AltCS,Arabinose,Glip,Xylose
PGI1	MIR1	-0.5	Glycls	MitTrnsp
PGI1	SOR1	-0.5	Glycls	AltCS
PGI1	FBA1	-0.5	Glycls	Glycls

Table S3. *(continued)*

G1	G2	iWT	G1 annotation	G2 annotation
SHM1	SHM2	-0.5	GlySer	GlySer
CTP1	MIR1	-0.5	MitTrnsp	MitTrnsp
APA1	PMP1	-0.5	Cys,PurPyr	ExtclTrnsp
TPI1	RPE1	-0.5	Glycls	PentPh
TPI1	MIR1	-0.5	Glycls	MitTrnsp
TPI1	ZWF1	-0.5	Glycls	PentPh
ALT2	MIR1	-0.5	AlaAsp	MitTrnsp
KGD2	MIR1	-0.5	TCAcycle,Glycls	MitTrnsp
LPD1	UGA1	-0.5	TCAcycle,GlySer,Glycls	Glu
LPD1	SER2	-0.5	TCAcycle,GlySer,Glycls	GlySer
LPD1	MIR1	-0.5	TCAcycle,GlySer,Glycls	MitTrnsp
LPD1	AAT1	-0.5	TCAcycle,GlySer,Glycls	AlaAsp,ArgPro,TyrTrpPhe
LPD1	SDH2	-0.5	TCAcycle,GlySer,Glycls	TCAcycle,OxPhos
LPD1	GAD1	-0.5	TCAcycle,GlySer,Glycls	Glu
LPD1	IDH1	-0.5	TCAcycle,GlySer,Glycls	TCAcycle
LPD1	SER1	-0.5	TCAcycle,GlySer,Glycls	GlySer,Pdx
LPD1	ALD6	-0.5	TCAcycle,GlySer,Glycls	TyrTrpPhe
LPD1	FUM1	-0.5	TCAcycle,GlySer,Glycls	OxPhos
SER2	SDH2	-0.5	GlySer	TCAcycle,OxPhos
SER2	FUM1	-0.5	GlySer	OxPhos
PFK1	RPE1	-0.5	Glycls	PentPh
PFK1	MIR1	-0.5	Glycls	MitTrnsp
PFK1	ZWF1	-0.5	Glycls	PentPh
LSC2	MIR1	-0.5	TCAcycle	MitTrnsp
RPE1	FBA1	-0.5	PentPh	Glycls
RPE1	ZWF1	-0.5	PentPh	PentPh
MIR1	FBA1	-0.5	MitTrnsp	Glycls
MIR1	MDH1	-0.5	MitTrnsp	OxPhos
MIR1	SDH2	-0.5	MitTrnsp	TCAcycle,OxPhos
MIR1	IDP2	-0.5	MitTrnsp	TCAcycle
MIR1	DIC1	-0.5	MitTrnsp	MitTrnsp
MIR1	ADH3	-0.5	MitTrnsp	Glip
MIR1	MDH2	-0.5	MitTrnsp	OxPhos
MIR1	ALD4	-0.5	MitTrnsp	OAA,TyrTrpPhe
MIR1	FUM1	-0.5	MitTrnsp	OxPhos
FBA1	ZWF1	-0.5	Glycls	PentPh
SDH2	SER1	-0.5	TCAcycle,OxPhos	GlySer,Pdx
SER1	FUM1	-0.5	GlySer,Pdx	OxPhos
COX1	PMP1	0.5	OxPhos	ExtclTrnsp
COX1	FUM1	0.5	OxPhos	OxPhos
ATP8	PMP1	0.5	OxPhos	ExtclTrnsp
ATP8	FUM1	0.5	OxPhos	OxPhos
COB	PMP1	0.5	OxPhos	ExtclTrnsp
COB	FUM1	0.5	OxPhos	OxPhos
GCV3	PGI1	0.5	Folate,GlySer	Glycls
GCV3	PMP1	0.5	Folate,GlySer	ExtclTrnsp
GCV3	TPI1	0.5	Folate,GlySer	Glycls

Table S3. *(continued)*

G1	G2	iWT	G1 annotation	G2 annotation
GCV3	ALT2	0.5	Folate,GlySer	AlaAsp
GCV3	PFK1	0.5	Folate,GlySer	Glycls
GCV3	RPE1	0.5	Folate,GlySer	PentPh
GCV3	MIR1	0.5	Folate,GlySer	MitTrnsp
GCV3	FBA1	0.5	Folate,GlySer	Glycls
GCV3	AAT1	0.5	Folate,GlySer	AlaAsp,ArgPro,TyrTrpPhe
ACH1	ALT2	0.5	Pyr	AlaAsp
ACH1	ALD6	0.5	Pyr	TyrTrpPhe
ACH1	FUM1	0.5	Pyr	OxPhos
PGI1	PMP1	0.5	Glycls	ExtclTrnsp
PGI1	SER2	0.5	Glycls	GlySer
PGI1	AAT1	0.5	Glycls	AlaAsp,ArgPro,TyrTrpPhe
PGI1	SER1	0.5	Glycls	GlySer,Pdx
PMP1	TPI1	0.5	ExtclTrnsp	Glycls
PMP1	ALT2	0.5	ExtclTrnsp	AlaAsp
PMP1	GLY1	0.5	ExtclTrnsp	ThrLys
PMP1	LPD1	0.5	ExtclTrnsp	TCAcycle,GlySer,Glycls
PMP1	SER2	0.5	ExtclTrnsp	GlySer
PMP1	PFK1	0.5	ExtclTrnsp	Glycls
PMP1	MIR1	0.5	ExtclTrnsp	MitTrnsp
PMP1	FBA1	0.5	ExtclTrnsp	Glycls
PMP1	AAT1	0.5	ExtclTrnsp	AlaAsp,ArgPro,TyrTrpPhe
PMP1	SER1	0.5	ExtclTrnsp	GlySer,Pdx
IDP1	AAT1	0.5	TCAcycle	AlaAsp,ArgPro,TyrTrpPhe
TPI1	ALT2	0.5	Glycls	AlaAsp
TPI1	LPD1	0.5	Glycls	TCAcycle,GlySer,Glycls
TPI1	SER2	0.5	Glycls	GlySer
TPI1	SER1	0.5	Glycls	GlySer,Pdx
ALT2	LPD1	0.5	AlaAsp	TCAcycle,GlySer,Glycls
ALT2	PFK1	0.5	AlaAsp	Glycls
ALT2	FBA1	0.5	AlaAsp	Glycls
ALT2	MET22	0.5	AlaAsp	Cys
ALT2	FUM1	0.5	AlaAsp	OxPhos
GLY1	MIR1	0.5	ThrLys	MitTrnsp
LPD1	PFK1	0.5	TCAcycle,GlySer,Glycls	Glycls
LPD1	RPE1	0.5	TCAcycle,GlySer,Glycls	PentPh
LPD1	FBA1	0.5	TCAcycle,GlySer,Glycls	Glycls
SER2	PFK1	0.5	GlySer	Glycls
SER2	RPE1	0.5	GlySer	PentPh
SER2	FBA1	0.5	GlySer	Glycls
SER2	AAT1	0.5	GlySer	AlaAsp,ArgPro,TyrTrpPhe

Table S3. *(continued)*

G1	G2	iWT	G1 annotation	G2 annotation
PFK1	SER1	0.5	Glycls	GlySer,Pdx
RPE1	MIR1	0.5	PentPh	MitTrnsp
RPE1	SER1	0.5	PentPh	GlySer,Pdx
MIR1	AAT1	0.5	MitTrnsp	AlaAsp,ArgPro,TyrTrpPhe
FBA1	SER1	0.5	Glycls	GlySer,Pdx
AAT1	SER1	0.5	AlaAsp,ArgPro,TyrTrpPhe	GlySer,Pdx
AAT1	ALD6	0.5	AlaAsp,ArgPro,TyrTrpPhe	TyrTrpPhe
COX1	ATP8	1	OxPhos	OxPhos
COX1	COB	1	OxPhos	OxPhos
COX1	PGI1	1	OxPhos	Glycls
COX1	IDP1	1	OxPhos	TCAcycle
COX1	MIR1	1	OxPhos	MitTrnsp
ATP8	COB	1	OxPhos	OxPhos
ATP8	GCV3	1	OxPhos	Folate,GlySer
ATP8	PGI1	1	OxPhos	Glycls
ATP8	IDP1	1	OxPhos	TCAcycle
ATP8	SER2	1	OxPhos	GlySer
ATP8	MIR1	1	OxPhos	MitTrnsp
ATP8	AAT1	1	OxPhos	AlaAsp,ArgPro,TyrTrpPhe
ATP8	SER1	1	OxPhos	GlySer,Pdx
ATP8	ALD6	1	OxPhos	TyrTrpPhe
COB	PGI1	1	OxPhos	Glycls
COB	IDP1	1	OxPhos	TCAcycle
COB	MIR1	1	OxPhos	MitTrnsp
GCV3	LPD1	1	Folate,GlySer	TCAcycle,GlySer,Glycls
PGI1	LPD1	1	Glycls	TCAcycle,GlySer,Glycls
IDP1	MIR1	1	TCAcycle	MitTrnsp
IDP1	ALD6	1	TCAcycle	TyrTrpPhe
SER2	MIR1	1	GlySer	MitTrnsp
SER2	SER1	1	GlySer	GlySer,Pdx
PFK1	FBA1	1	Glycls	Glycls
MIR1	SER1	1	MitTrnsp	GlySer,Pdx
MIR1	ALD6	1	MitTrnsp	TyrTrpPhe

Table S3. *(continued)*

Subgroup (control)	Test group	Mean instability	p-value
Strong	Intra-group	2.7	2.3×10^{-5}
	Inter-group	5.1	
Weak	Intra-group	8.3	0.97
	Inter-group	8.7	
Strong	Positive	7.1	2.1×10^{-9}
	Negative	2.4	
Weak	Positive	10.9	1.8×10^{-7}
	Negative	7.1	
Intra-group	Positive	7.1	0.013
	Negative	4.2	
Inter-group	Positive	10.3	1.78×10^{-10}
	Negative	6.0	
Intra-group	Strong	2.7	9.7×10^{-8}
	Weak	8.3	
Inter-group	Strong	5.1	$1.9 \times 10{-}7$
	Weak	8.7	
Positive	Intra-group	7.1	0.014
	Inter-group	10.3	
Negative	Intra-group	4.2	0.002
	Inter-group	6.0	
Positive	Strong	7.1	1.8×10^{-4}
	Weak	10.9	
Negative	Strong	2.4	5.2×10^{-18}
	Weak	7.1	

Table S4. Genetic interaction stability as a function of sign, strength and functional association.

Gene	Pleiotropy	Annotation
TPI1	41	Glycls
PFK1	41	Glycls
FBA1	41	Glycls
COX1	39	OxPhos
ATP8	39	OxPhos
COB	39	OxPhos
MIR1	34	Mit. Trnsp
PGI1	30	Glycls
PMP1	28	Extcl. Trnsp
SER2	28	GlySer
SER1	28	GlySer, Pyridoxine
RPE1	27	PentosePhosphate
GCV3	23	Folate,GlySer
LPD1	23	TCA cycle,GlySer,Glycls
ACH1	14	Pyruvate
ALD6	12	TyrTrpPhe
FUM1	11	OxPhos
AAT1	3	AlaAsp,ArgPro,TyrTrpPhe
APA1	2	Cys,PurPyr
IDP1	2	TCA cycle
ALT2	2	AlaAsp
GLY1	2	ThrLys
PSD1	2	Plip
MET22	2	Cysteine,
PRO1	1	ArgPro
DCD1	1	Nuc. Salv.PurPyr
ADO1	1	Nuc. Salv.
PRO2	1	ArgPro

Table S5. Pleiotropy is present in catabolic genes and absent in biosynthetic ones.

Full name	Abreviated name
Alternate Carbon Metabolism	Alt. CS
Transport Mitochondrial	Mit. Trnsp
Tyrosine Tryptophan and Phenylalanine Metabolism	Tyr,Trp,Phe
Arginine and Proline Metabolism	Arg, Pro
Threonine and Lysine Metabolism	Thr, Lys
Transport Extracellular	Extcl. Trnsp
Other Amino Acid Metabolism	OAA
Glutamate metabolism	Glu
Valine Leucine and Isoleucine Metabolism	Val,Leu,Ile
Pyruvate Metabolism	Pyr
Citric Acid Cycle	TCA cycle
Nucleotide Salvage Pathway	Nuc. Salv.
Folate Metabolism	Folate
Phospholipid Biosynthesis	Plip
Purine and Pyrimidine Biosynthesis	Pur,Pyr
Cysteine Metabolism	Cys
Glycine and Serine Metabolism	Gly,Ser
Methionine Metabolism	Met
Alanine and Aspartate Metabolism	Ala,Asp
Glycerolipid Metabolism	Glip
Arabinose Metabolism	Ara
Oxidative Phosphorylation	OxPhos
Glycolysis and Gluconeogenesis	Glycls
Pentose Phosphate Pathway	Pent. Ph.
Anaplerotic reactions	Anapl.
Pyridoxine Metabolism	Pdx

Table S6. Notation of metabolic modules associated to Fig. 2, main manuscript, that is also used thoughout the supplement.

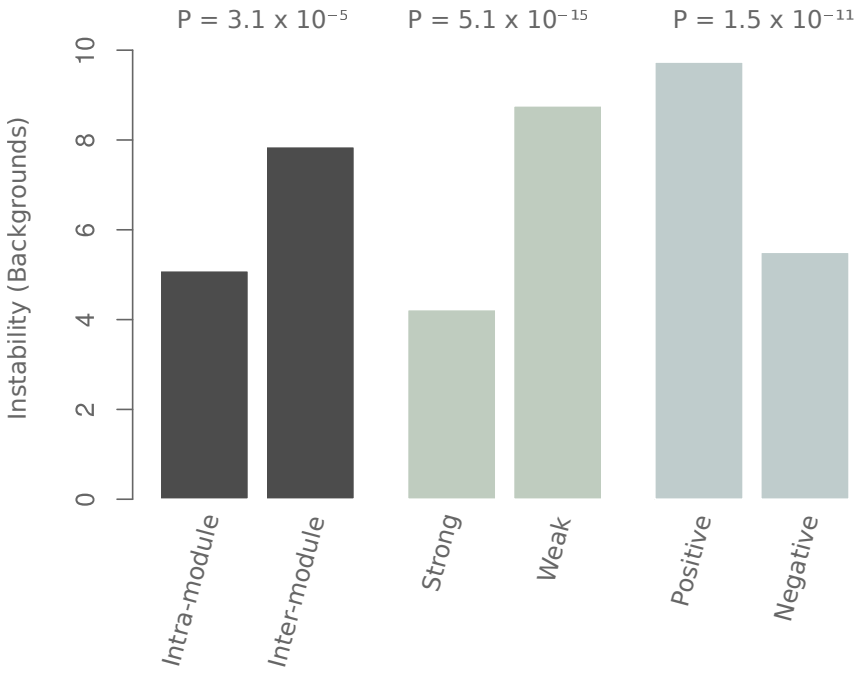

Figure S1. Differential stability of interactions: influence of metabolic distribution, strength, and sign. Differential stability of WT interactions with respect to whether their constituents genes belong to the same metabolic module (intra-module *vs.* inter-module; left), interaction strength (strong *vs.* weak; center) and type (positive *vs.* negative; right). For each interaction, instability was computed as the number of backgrounds where it disappears, changes sign, strength or both. In this figure, bars represent averages (p-values shown on top were obtained using the wilcoxon test between each pair of groups).

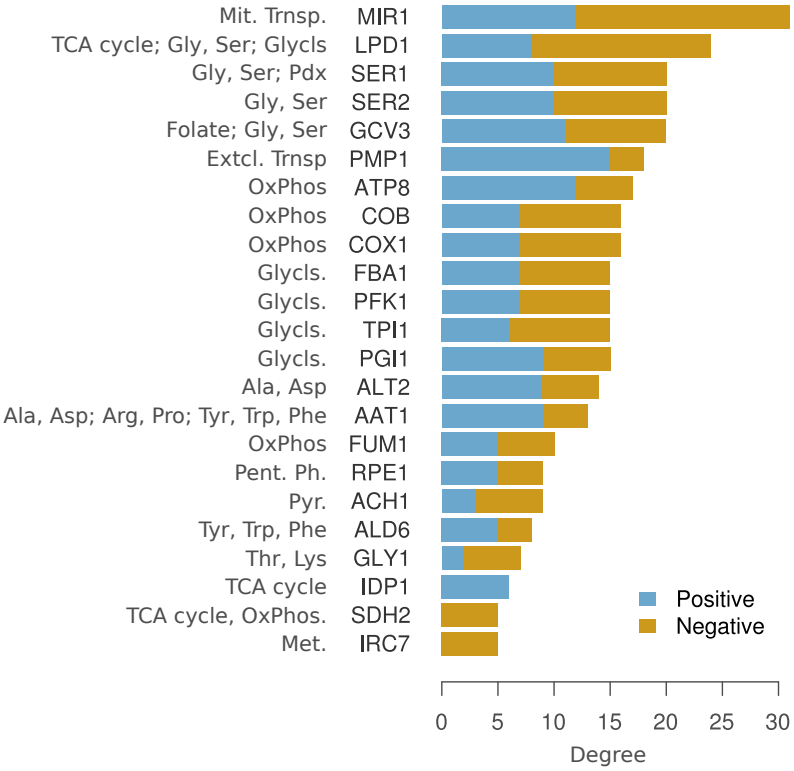

Figure S2. Genetic hubs in the WT `iND750` metabolism of *S. cerevisiae*. We depict here the degrees of the top 25 most connected genes (this is the list of genetic hubs considered in the manuscript). Colors indicate the proportion of negative and positive interactions.

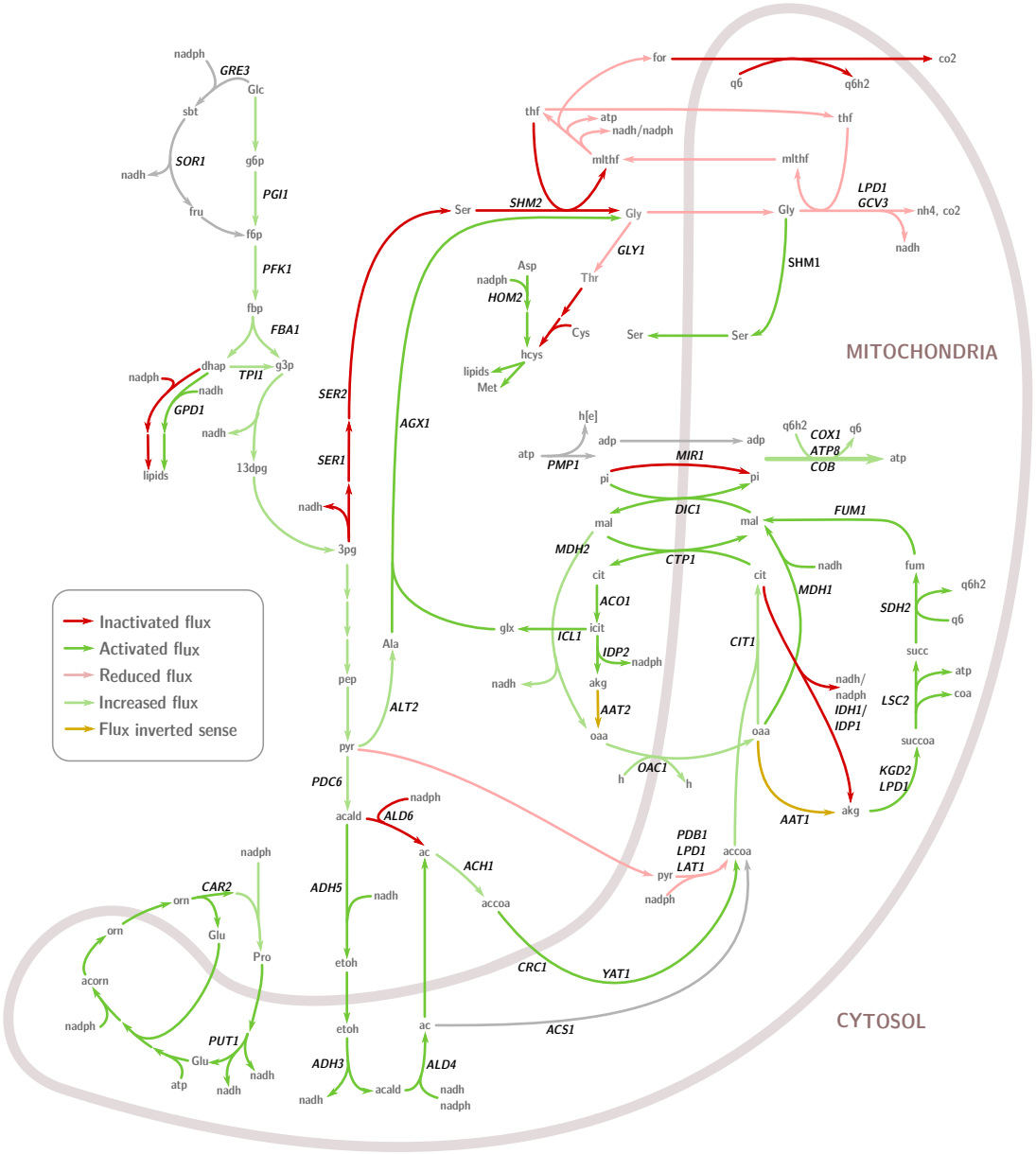

Figure S3. Schematical representation of the metabolic changes that occur upon `MIR1` deletion. Colors indicate whether a given flux has increased, decreased, shut off or on, or changed direction, as shown in the legend.

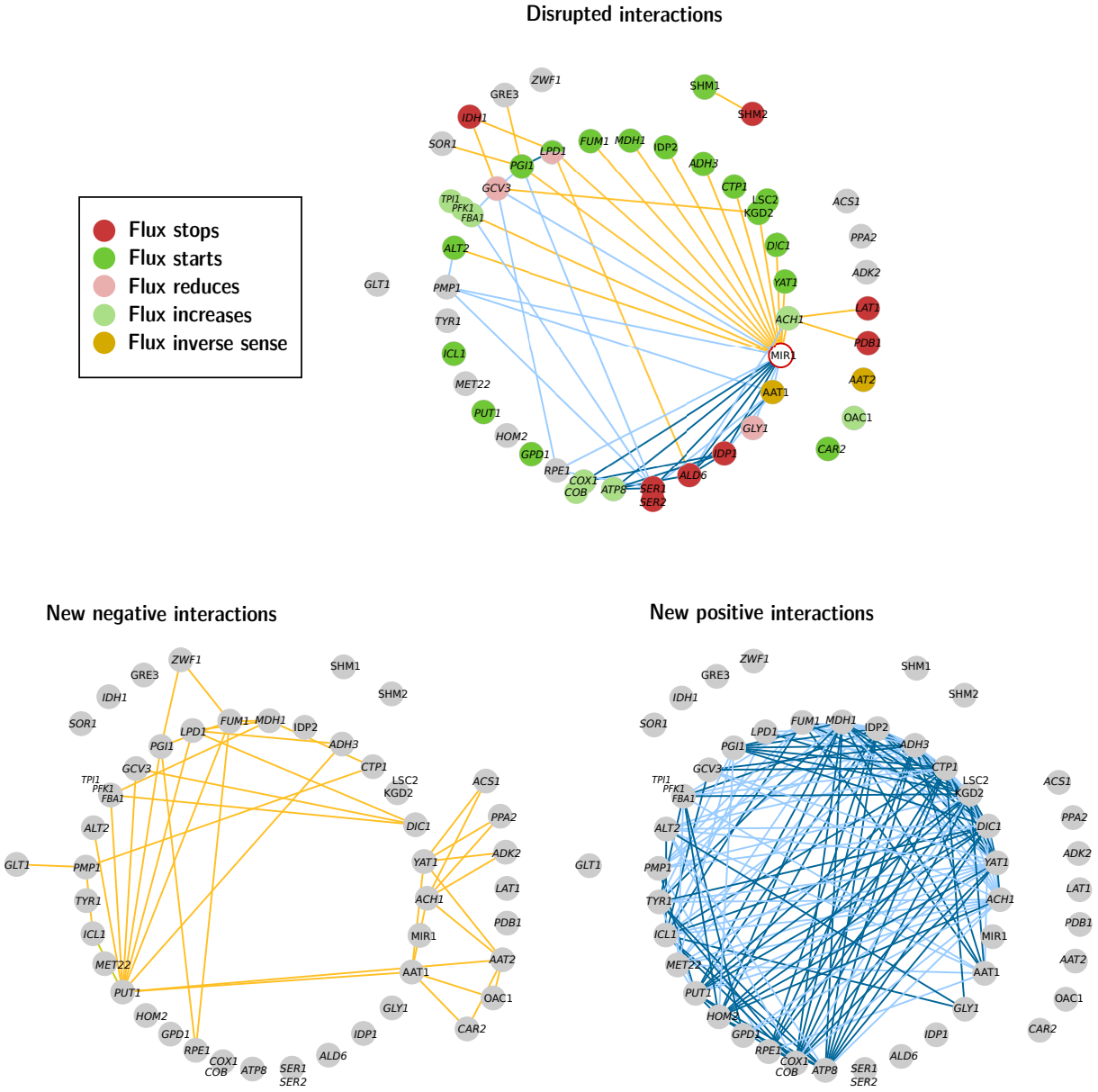

Figure S4. Rewiring of genetic interactions in `MIR1` background (Δ`MIR1`). Top: disrupted negative (yellow) and positive (blue) interactions. Node color represents the metabolic effect of the deletion on the reaction(s) associated to the node (see legend). Almost all the lost interactions involve either the background gene or genes that interact positively with it. Bottom-left: new negative interactions. Bottom-right: new positive interactions.

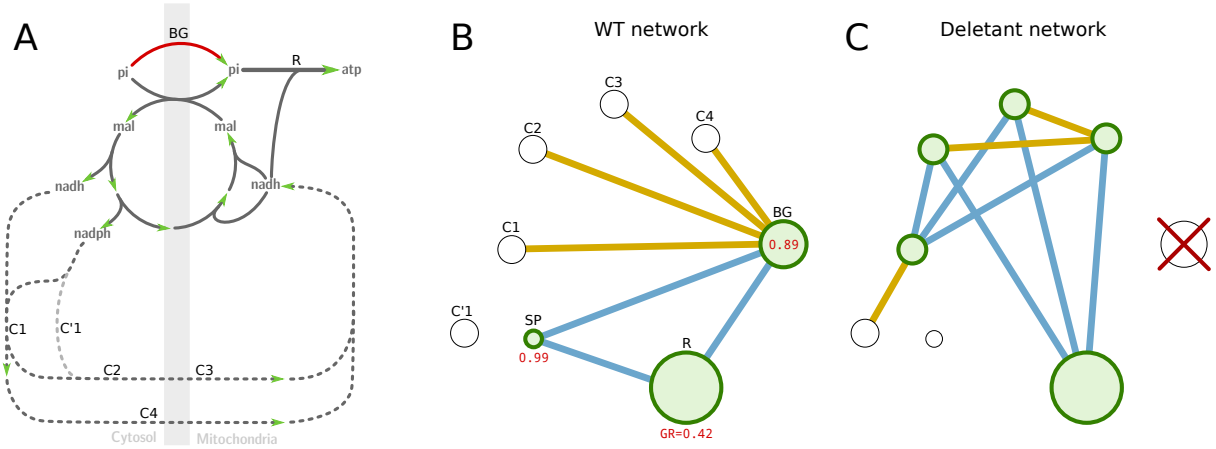

Figure S5. A) Schematic summary of metabolic and genetic changes after a background deletion. The cartoon is based on the Δ`MIR1` background, but aiming to provide a description of the general principles of genetic rewiring, and how it reflects metabolic changes. A) Upon deletion of a background gene (BG), a compensatory mechanism is activated (`C1`). This compensation usually originate side effects (in the case of `MIR1`, extrusion of malate from mitochondria) unless it is fully equivalent (e.g., duplicated genes). Additional mechanisms are thus activated to correct these secondary imbalances (`C1`, `C2`, `C3`, and `C4`, dashed lines). B) WT genetic network, with nodes associated to flux-carrying reactions colored green, and single fitness contribution as node size. BG interacts negatively (yellow) with compensatory mechanisms (`C1`, `C2`, `C3`, `C4`). Positive interactions (blue) occur either with the targets of its function (e.g., with respiration, R, as it is the ultimate target of phosphate import to mitochondria) or with genes that stop functioning when BG is compromised (generally displaying lower fitness effect thang BG; SP for strong positive partner). C) In the mutated network, the target mechanism (respiration) interacts positively with those genes that compensate for the BG deletion (`C1`, `C2`). These compensatory mechanisms can interact among them positively or negatively, depending on the underlying functional relationship. Some of them can have in turn their own compensating mechanisms in the new background (e.g., `C'1` buffers `C1`) also producing new negative interactions.

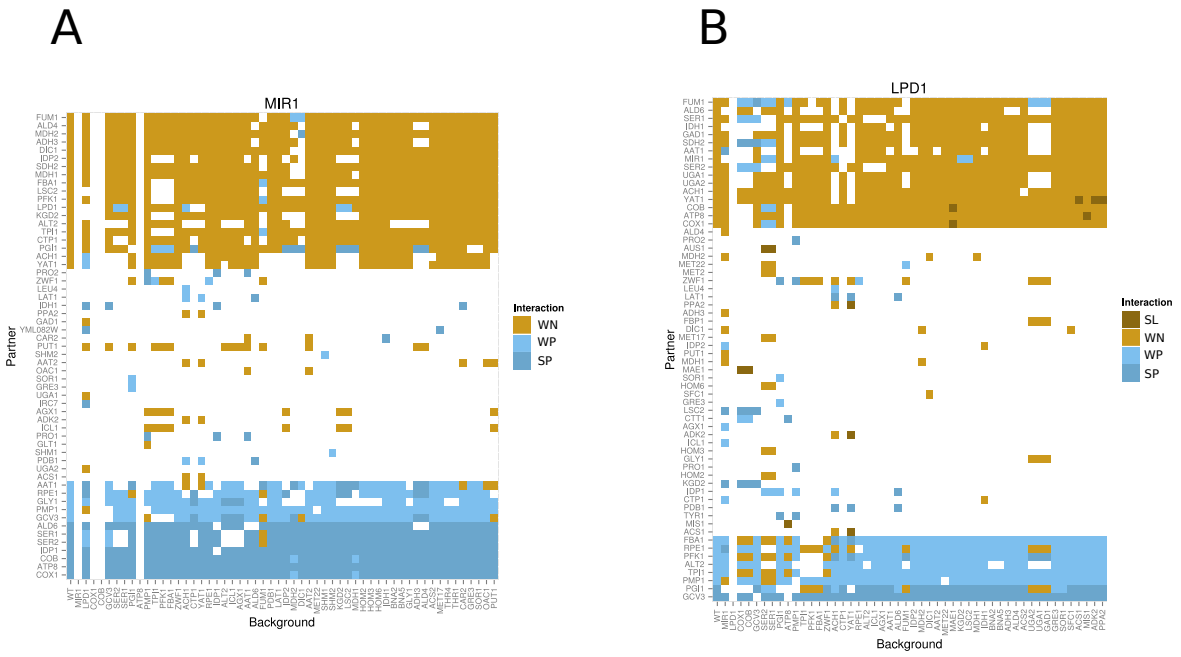

Figure S6. Rewiring of hubs MIR1 (A) and LPD1 (B) in all backgrounds. Figures equivalent to Fig. 4A, main text.

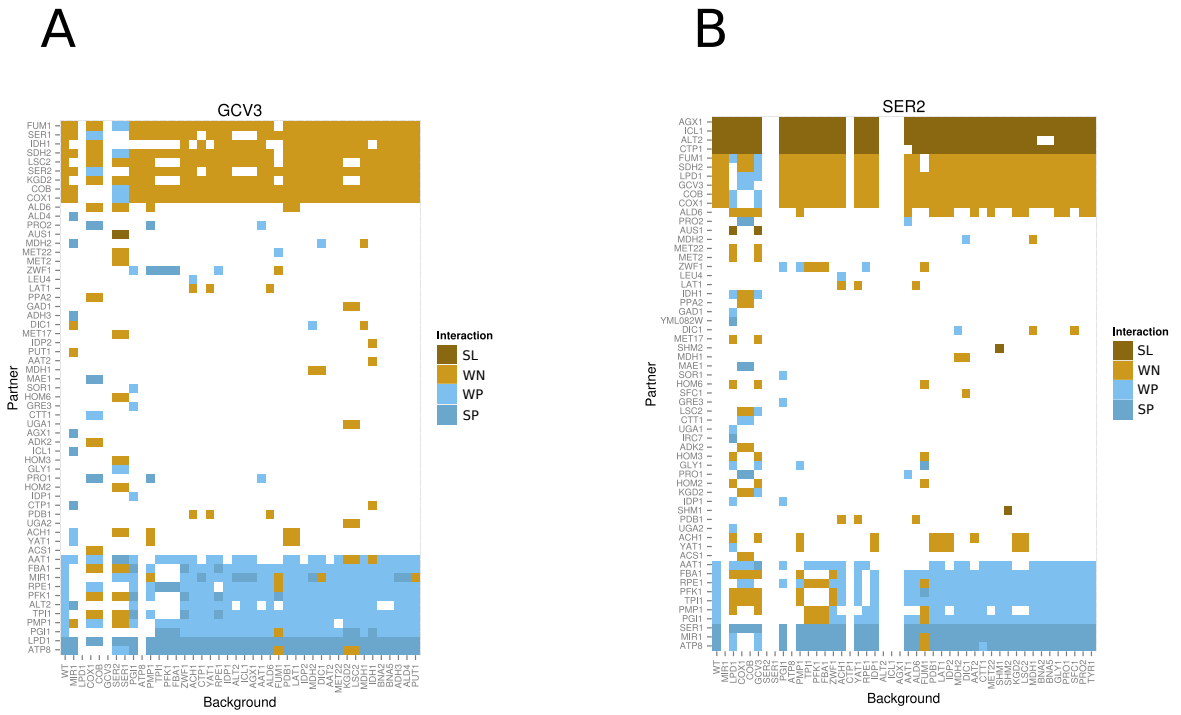

Figure S7. Rewiring of hubs GCV3 (A) and SER2 (B) in all backgrounds. Figures equivalent to Fig. 4A, main text.

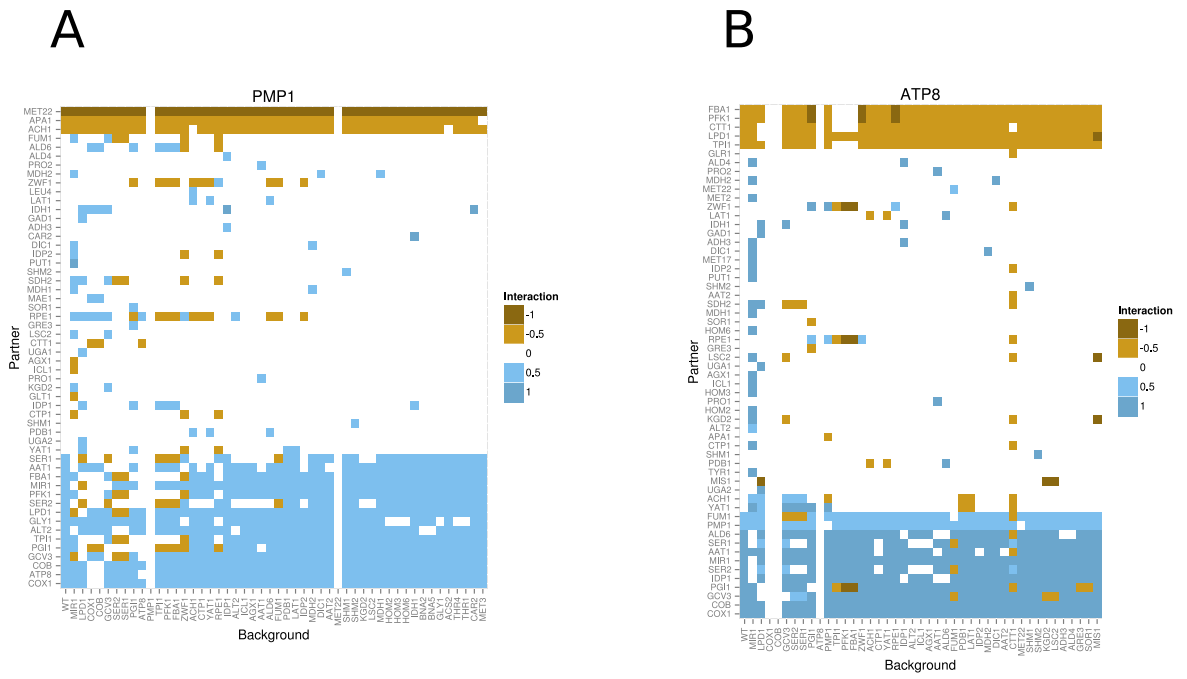

Figure S8. Rewiring of hubs PMP1 (A) and ATP8 (B) in all backgrounds. Figures equivalent to Fig. 4A, main text.

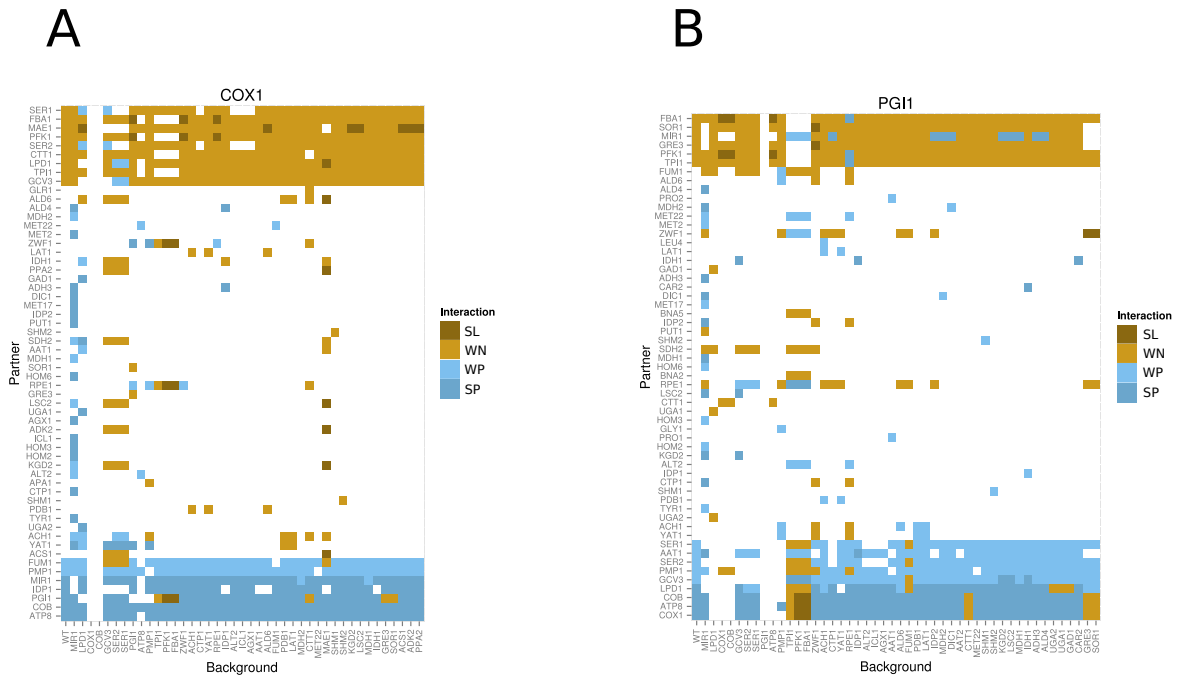

Figure S9. Rewiring of hubs COX1 (A) and PGI1 (B) in all backgrounds. Figures equivalent to Fig. 4A, main text.

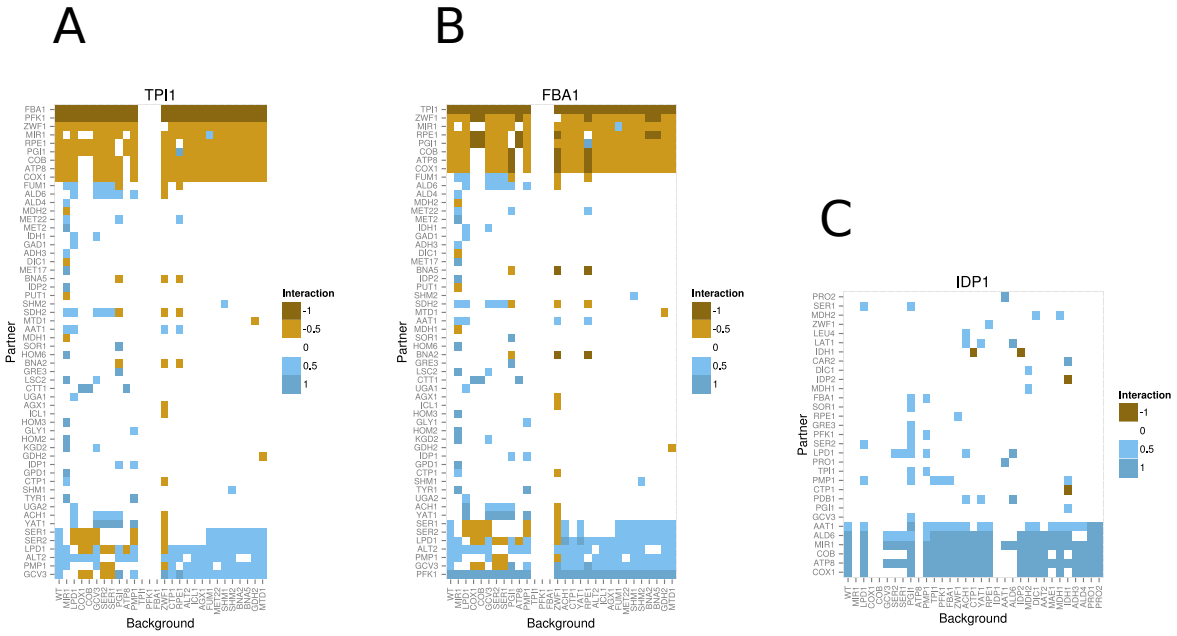

Figure S10. Rewiring of hubs TPI1 (A), FBA1 (B) and IDP1 (C) in all backgrounds. Figures equivalent to Fig. 4A, main text.

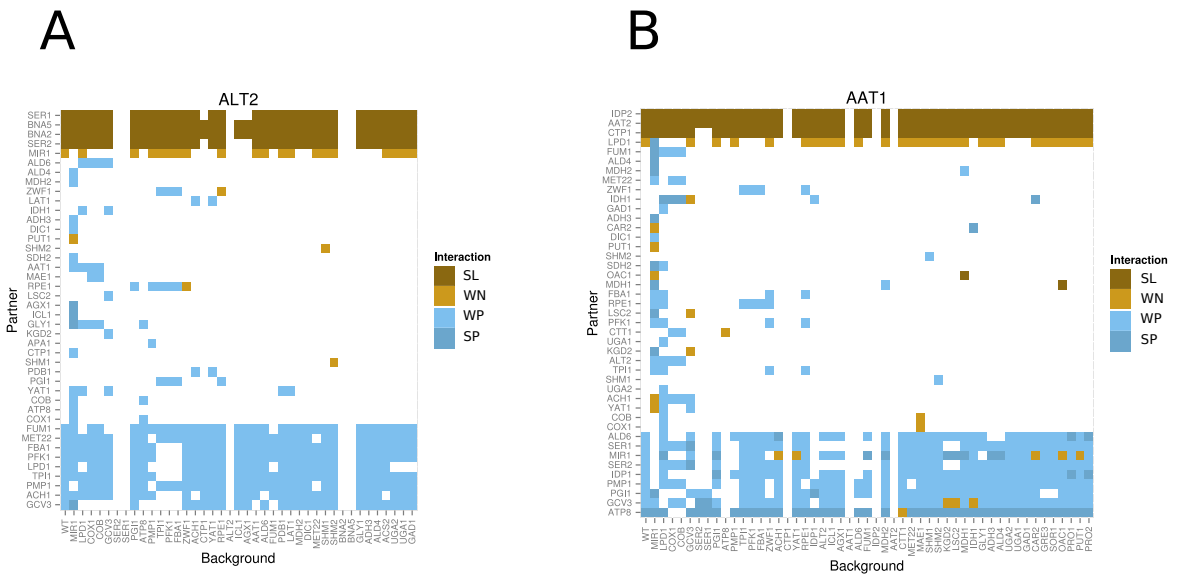

Figure S11. Rewiring of hubs ALT2 (A) and AAT1 (B) in all backgrounds. Figures equivalent to Fig. 4A, main text.

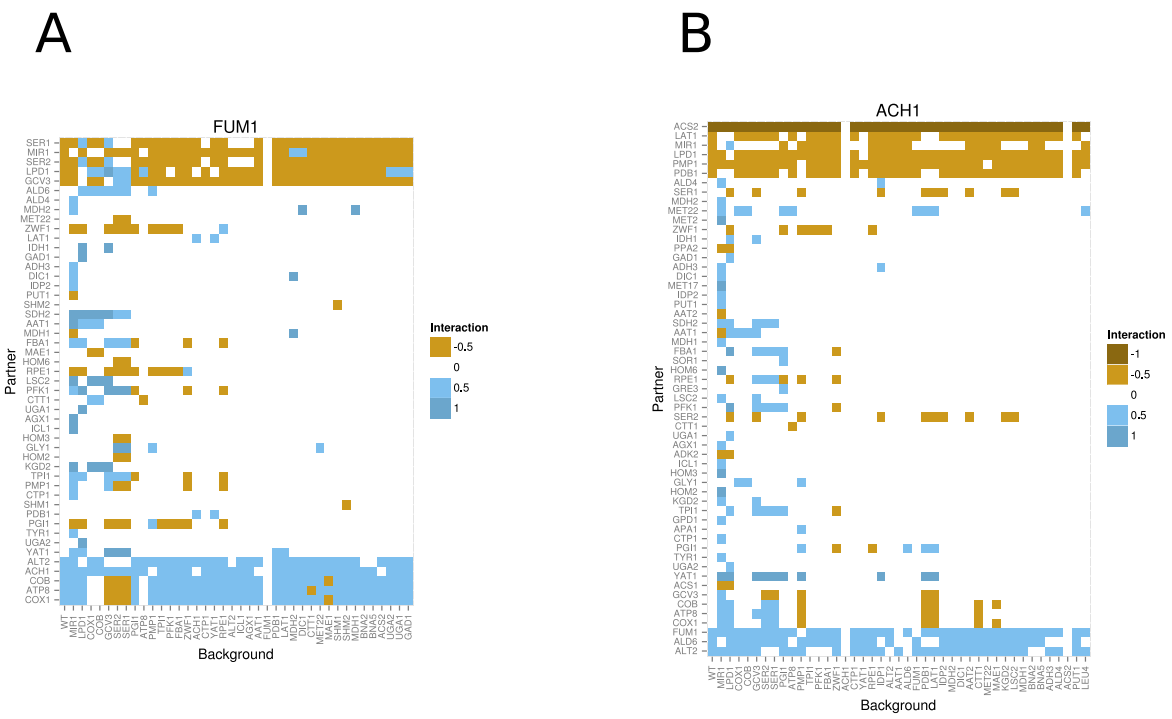

Figure S12. Rewiring of hubs FUM1 (A) and ACH1 (B) in all backgrounds. Figures equivalent to Fig. 4A, main text.

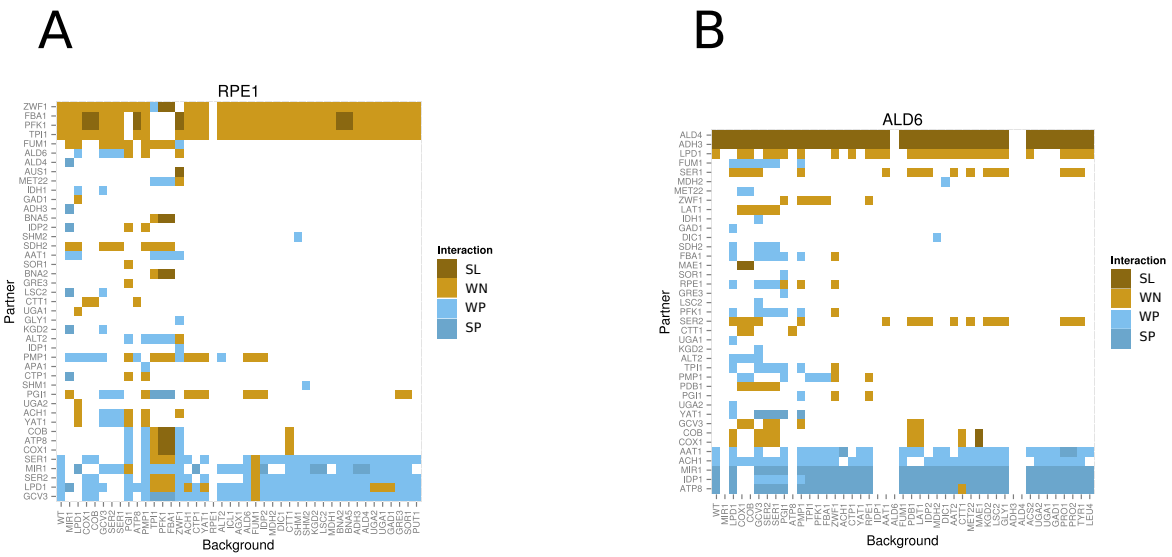

Figure S13. Rewiring of hubs RPE1 (A) and ALD6 (B) in all backgrounds. Figures equivalent to Fig. 4A, main text.

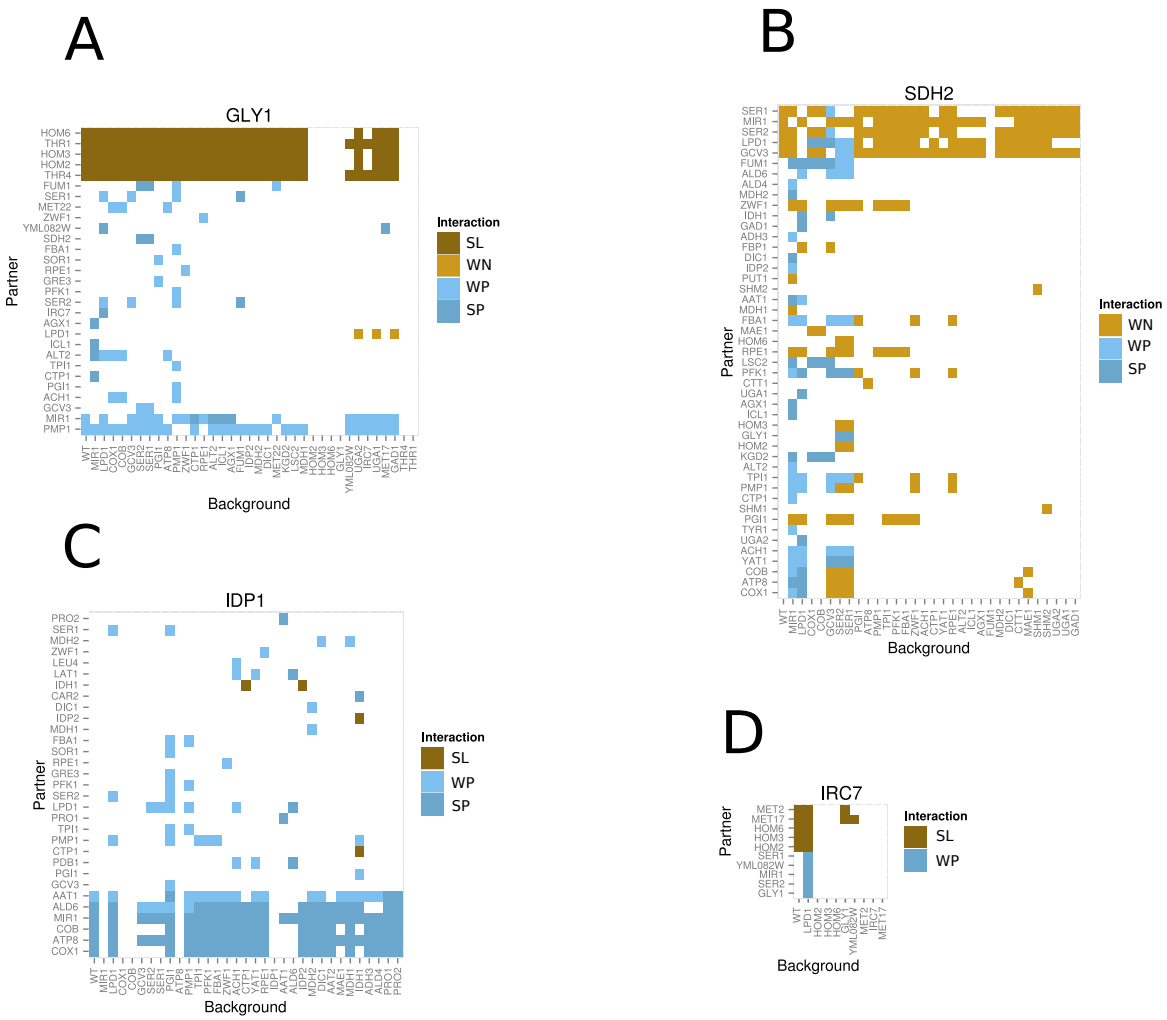

Figure S14. Rewiring of hubs GLY1 (A), SDH2 (B), IDP1(C) and IRC7 (D) in all backgrounds. Figures equivalent to Fig. 4A, main text.

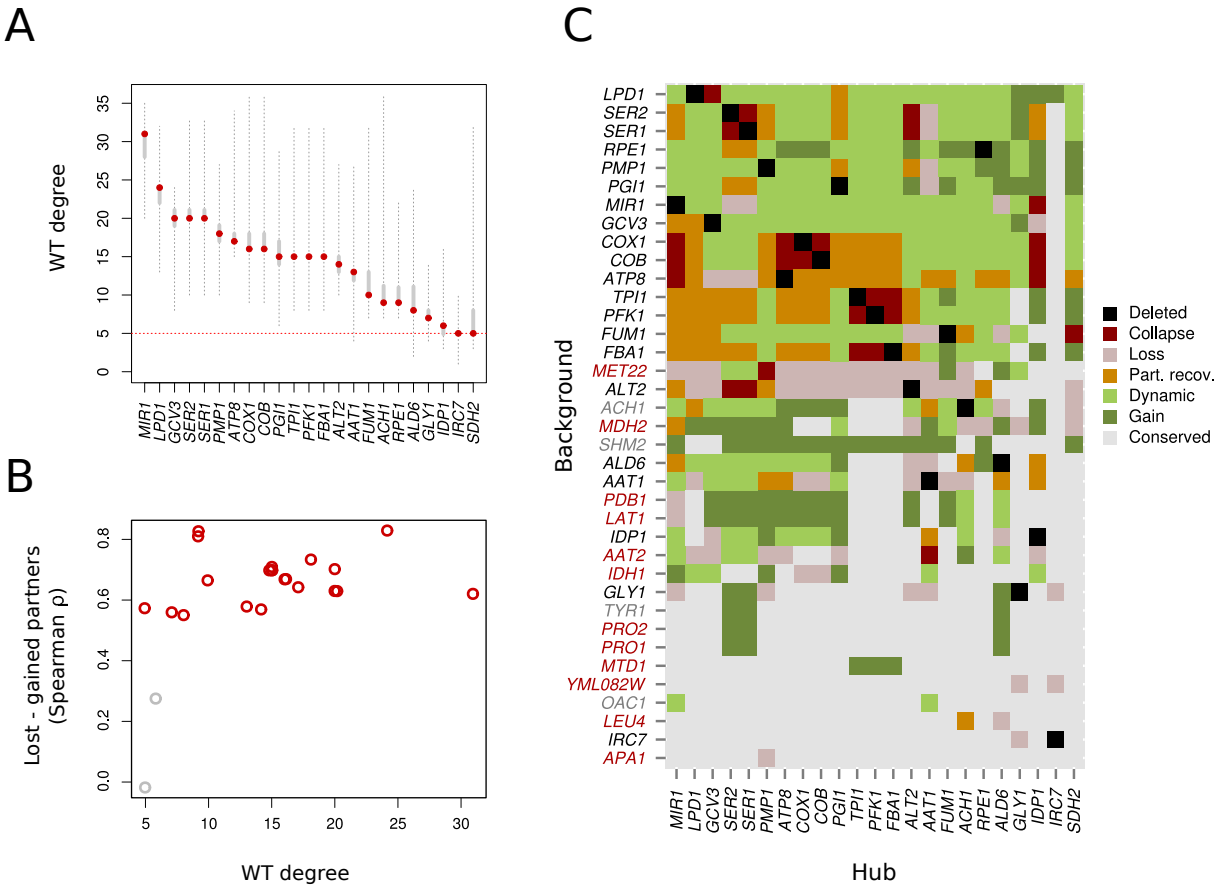

Figure S15. A) Distribution of the connectivity (degree) exhibited by each hub in each background. Red dots show the WT degree, thick gray lines illustrate percentile 10 to 90, and dashed lines represent the range from the minimum (nonzero) to the maximum degree values observed. B) Number of gained and (number of) conserved genetic interactions are negatively correlated in hubs (each dot represents the Spearman's correlation coefficient between lost WT interactions and newly gained ones; red color indicates P <0.001 significance). C) We classified the type of rewiring as (*horizontal*: 23 hubs, *vertical*: 37 backgrounds where they become unstable): "Collapse", if the hub lost all its interactions; "Loss", if it lost only part; "Partial recovery" if part of the missing genetic interactions were substituted by new ones; "Dynamic rewiring" if all of the lost interactions were substituted by new ones, so that the new degree is at least equal to that of the WT; "Gain" if the hub conserves the same partners as in the WT but gained additional ones. Moreover, "deleted" means that the node is the same as the background, and "conserved" means that the interactions of the node remain the same. Background names are colored black if they are as well hubs, red if they are not hubs in the WT but become a hub in at least one background, and gray if neither of these definitions apply.

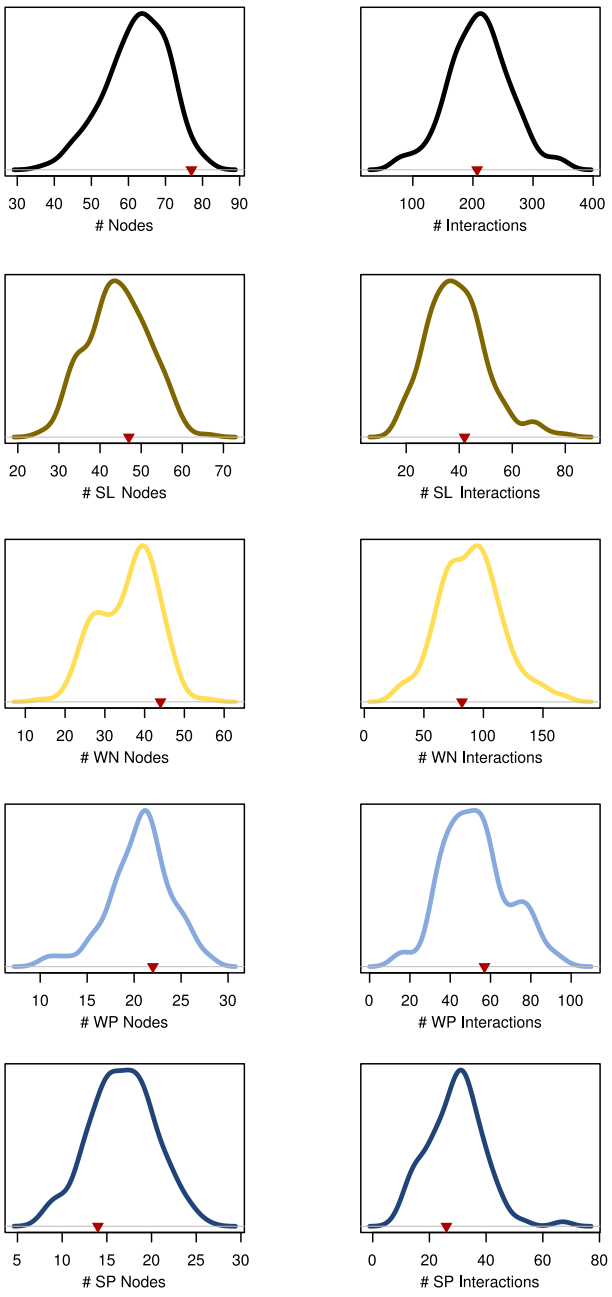

Figure S16. Distribution of the number of nodes and interactions, by interaction type, in the 200 genetic networks resulting from neutral deletion accumulation trajectories. Red triangles indicate WT values.

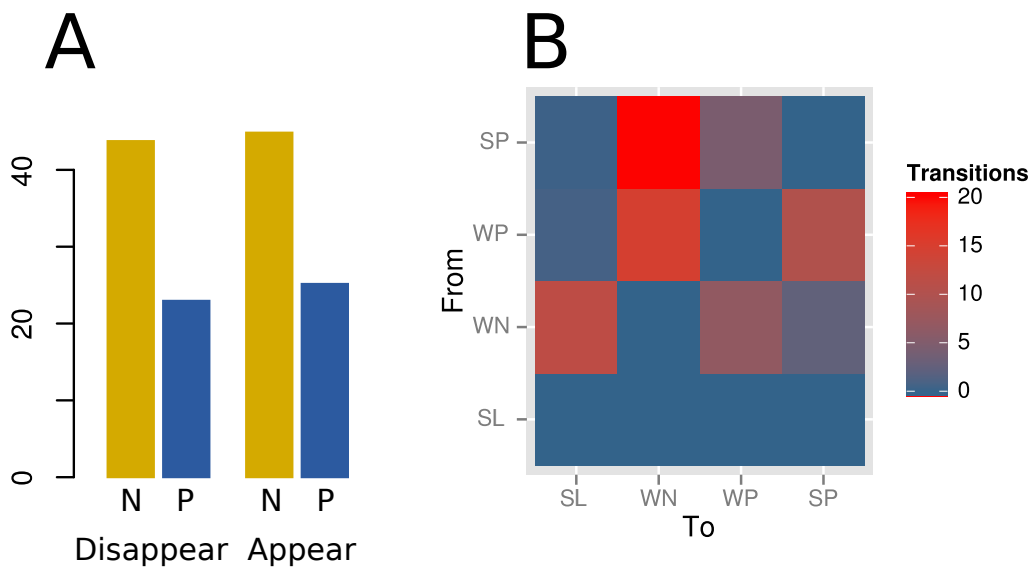

Figure S17. A) Average number of negative (N) and positive (P) interactions observed to disappear and appear in genetic networks in response to neutral backgrounds. B) Average number of transitions between interaction types observed when comparing these networks with the WT one. A stronger tendency to rewiring can be observed in negative interactions overall.

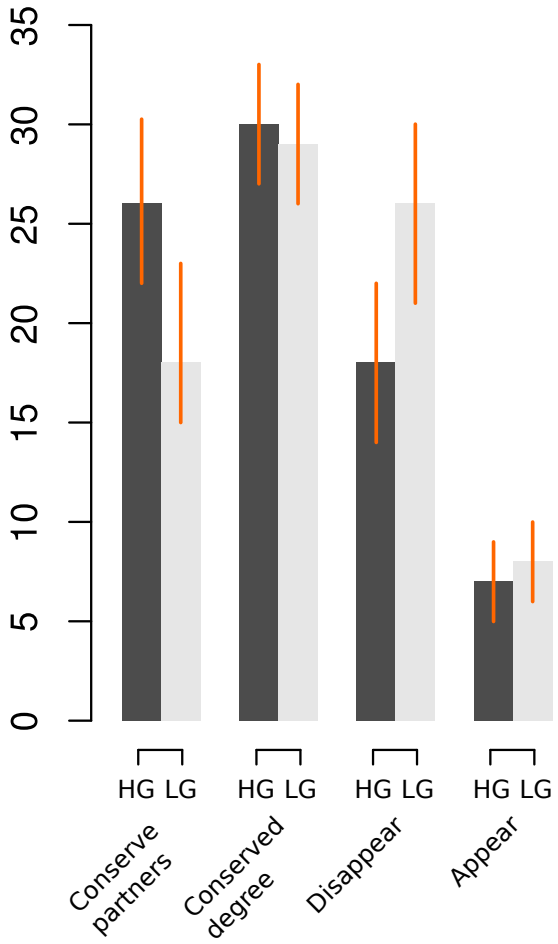

Figure S18. Differential rewiring in LG and HG backgrounds. We show (left to right): average number of nodes whose degree is conserved (all partners equal than in the WT), number of those that conserved degree but changed their partners, number of nodes that lost interactions, and number of nodes that gained interactions.

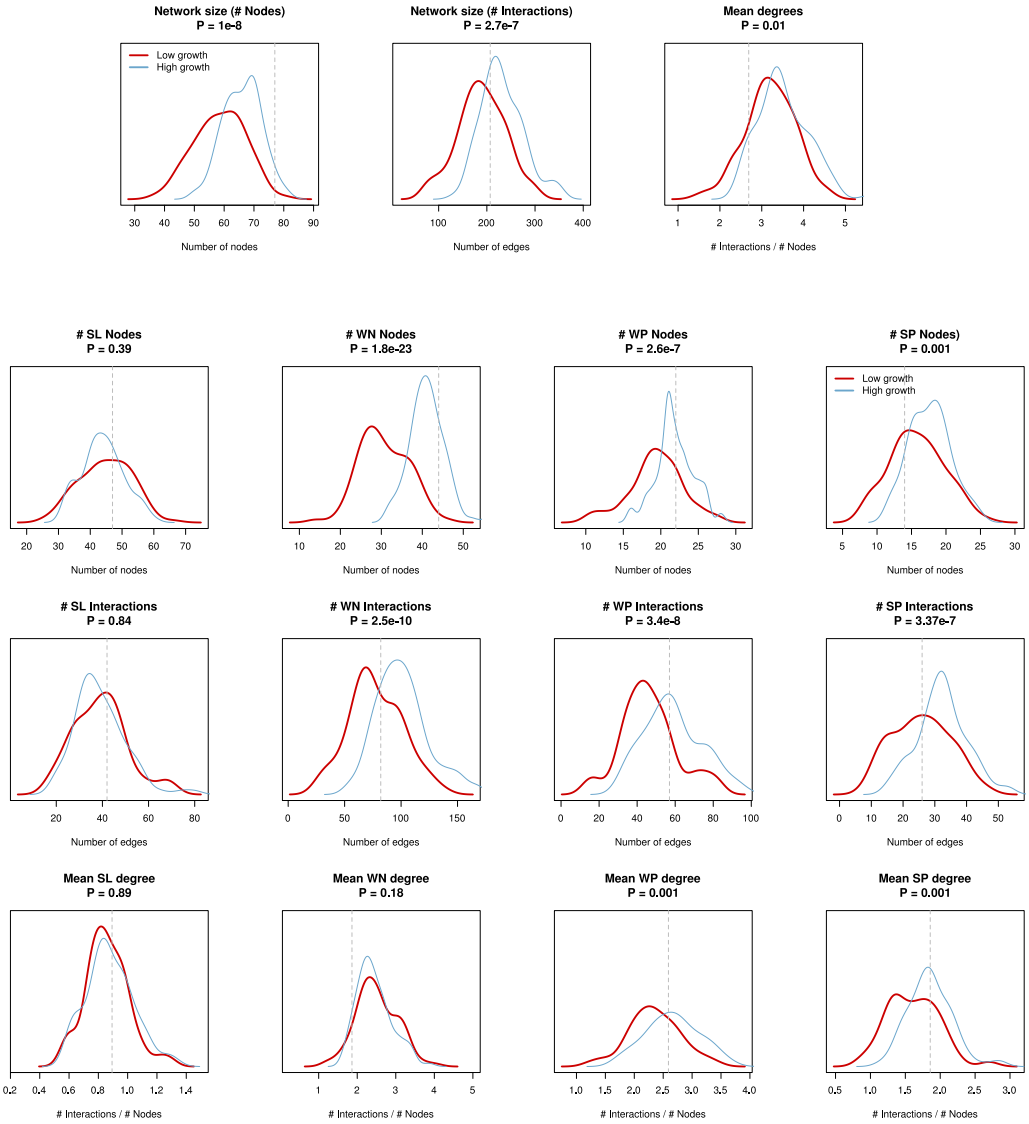

Figure S19. *Top:* distribution of number of interactions, number of nodes, and interactions/node for LG (red) and HG (blue) networks (neutral backgrounds). *Bottom:* as before but restricted to the subnetworks constituted by synthetic lethal (SL, left), weak negative (WN, middle-left), weak positive (WP, middle-right), and strong positive (SP, right) interactions.

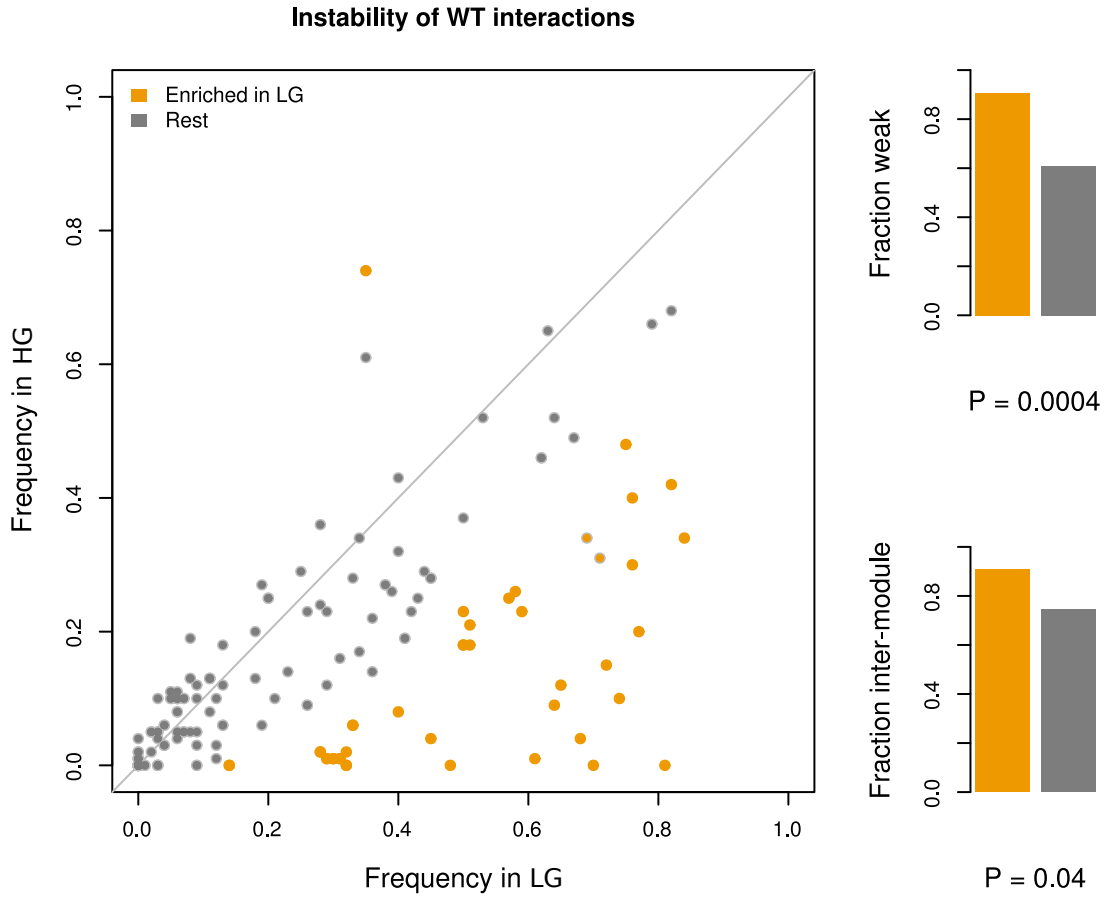

Figure S20. Frequency of LG and HG neutral trajectories in which a given WT interaction (dot) rewires (i.e., it dissappears, changes strength or sign). A) For each interaction, a p-value was obtained using Fisher's exact test (comparing the number of instabilities observed in HG and LG) and correction for multiple testing using the Benjamini-Hochberg-Yekutieli procedure [2]; those cases with $p < 0.001$ were colored in orange. B) Fraction of weak and inter-module interactions in the "LG-enriched" and "rest" subgroups.

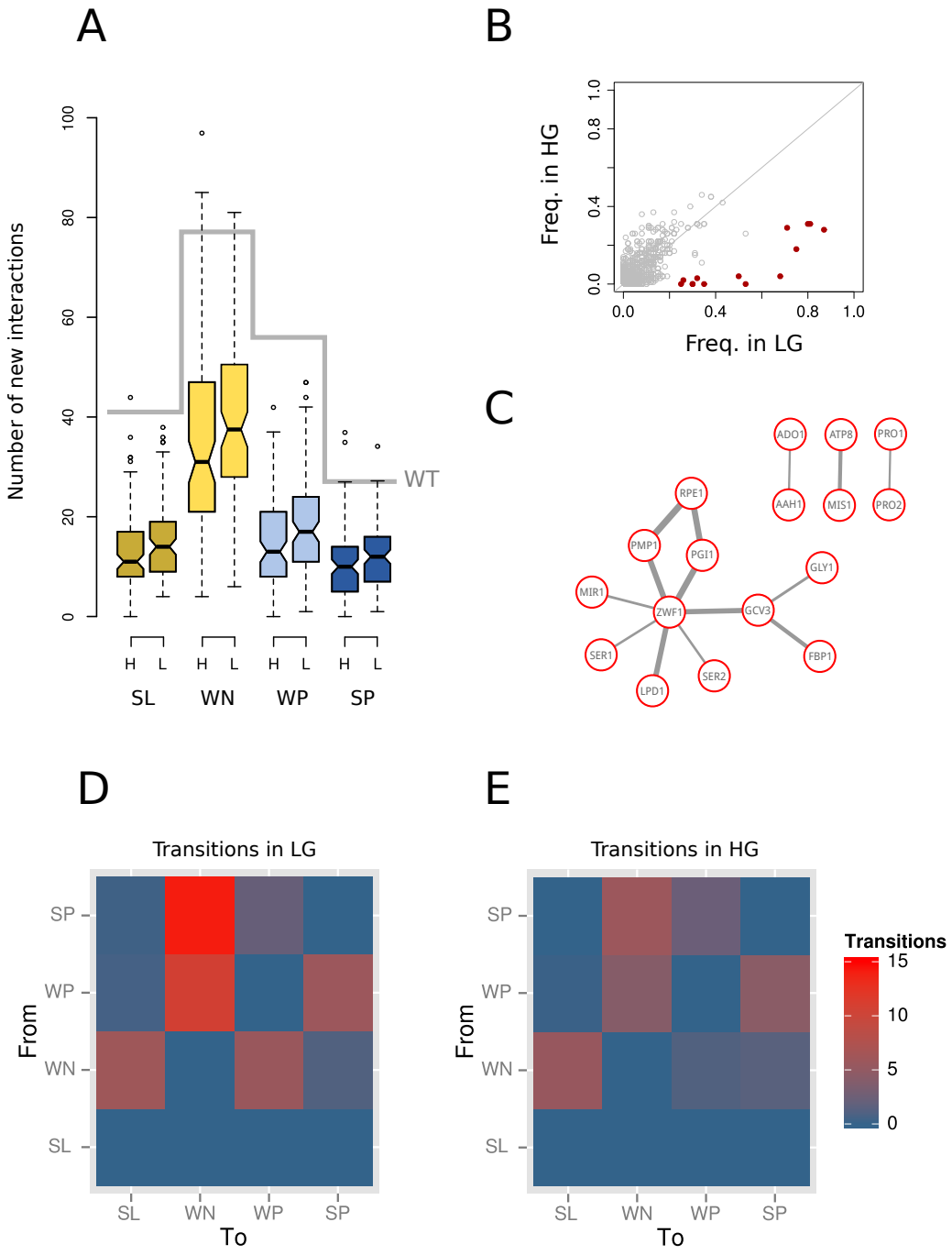

Figure S21. A) Distribution of the number of new interactions by type in LG (L) and HG (H) genotypes. For reference, we plotted the distribution of interactions in the WT network as a gray histogram line. B) For all unique interactions that appear in any of these genotypes, we plot its frequency in the HG and LG classes. We colored in red those interactions significantly enriched in LG networks (individual Fisher tests, p-values corrected for multiple testing using the Benjamini-Hochberg-Yekutieli procedure [2]). C) Interactions shown in red in B are represented here as a network (edge thickness is proportional to the frequency of each interaction). D) Transition map between types of interactions in LG, and E) in HG networks.

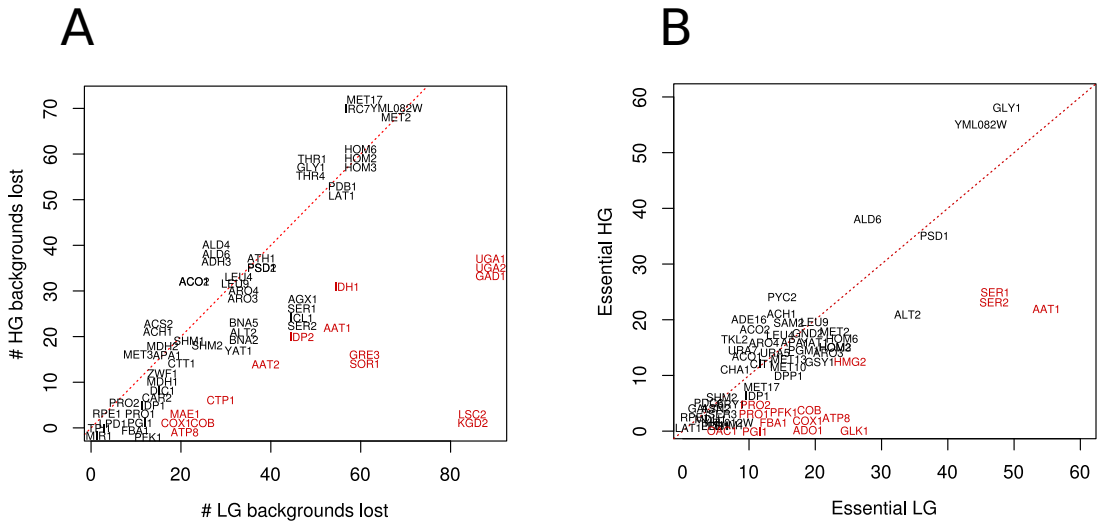

Figure S22. A) For each node in the WT network, we computed the frequency it disappears from the network in LG and HG genotypes (in red those nodes that are lost more frequently in LG). B) The same was done measuring the frequency at which genes become essential in LG and HG genotypes (in red those genes that become more frequently essential in LG).

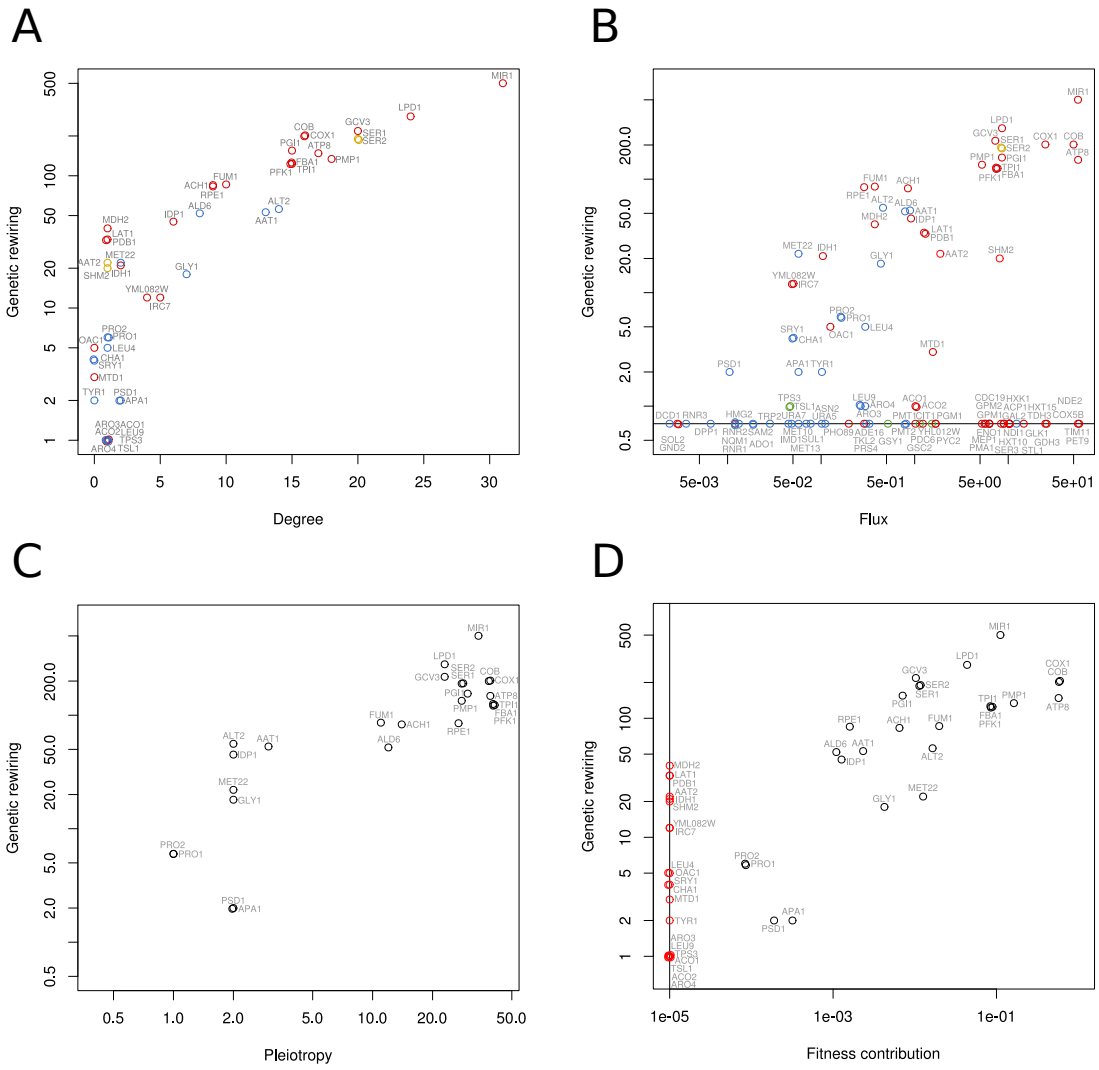

Figure S23. Correlation between genetic rewiring in different backgrounds and their A) degree, B) total flux through the associated reactions, C) pleiotropy, and D) single-gene fitness contribution.

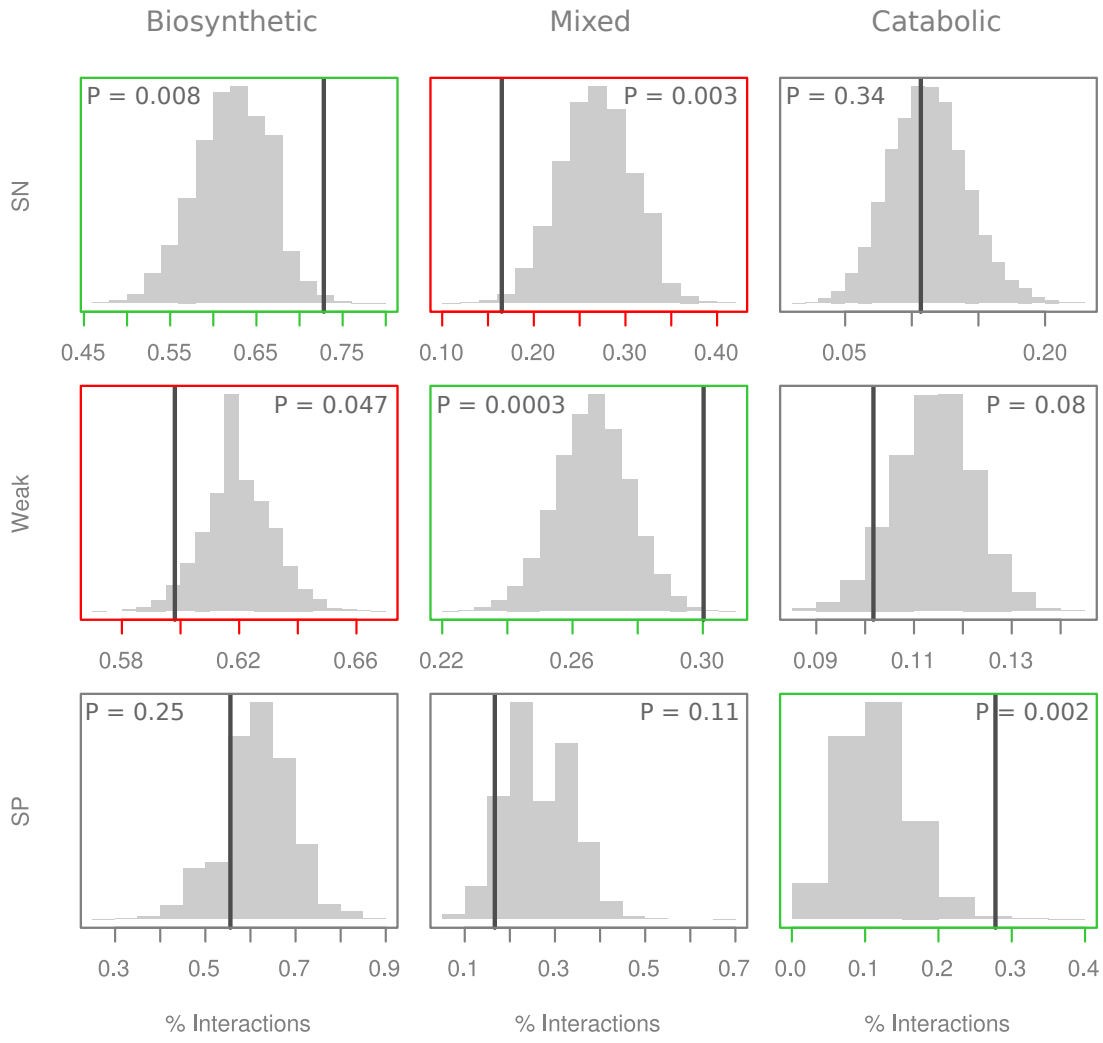

Figure S24. We selected from the high-confidence genetic interaction dataset in [3] those interactions between genes present in the `iND750` model of *S. cerevisiae*. We separated the dataset into strong positive (upper quartile among positive in strength), strong negative (idem among negative) and weak (the rest). For functional classification, we conservatively considered a gene as "catabolic" if it belongs to either glycolysis, TCA cycle or oxidative phosphorylation; the rest were considered "biosynthetic". According to this classification, an interaction can be catabolic, biosynthetic, or mixed (when one gene is catabolic and the other biosynthetic). In each strength category, we computed the percentage belonging to each functional class (vertical lines). To assess if any class is particularly enriched or depleted, we performed a bootstrapping analysis by randomizing 10000 times the assignment between strength and functional category of interactions. The distribution of percentages is shown in histograms, with the corresponding p-values. Plot boxes were colored red if significant depletion, and green if significant enrichment.

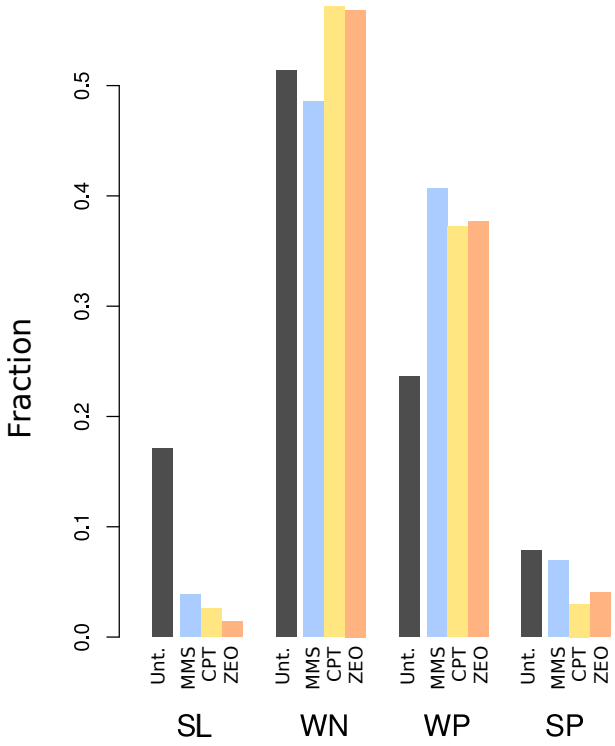

Figure S25. We computed, for all interactions appearing in at least one treatment, but not in the untreated network (i.e., treatment-specific interactions), the proportion of each strength/sign category. Treatment specific interactions are enriched in weak (especially weak positive) and depleted in strong (especially, in strong negative).

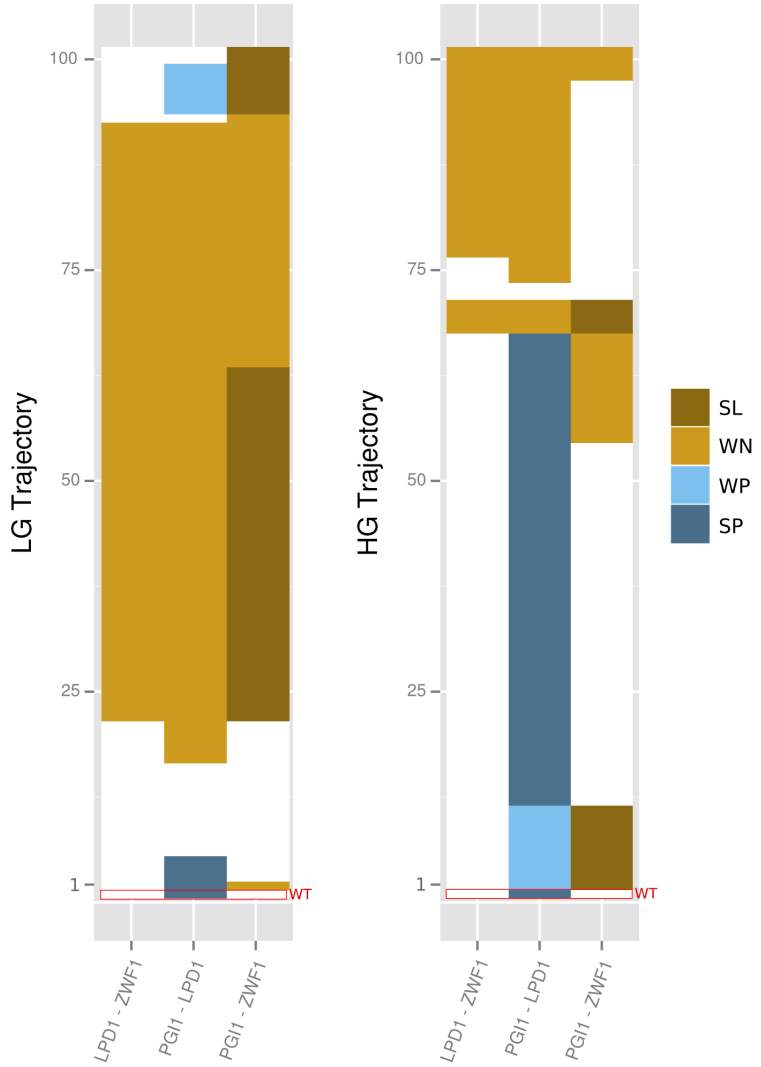

Figure S26. Genetic interactions between three genes representative of pentose phosphate pathway (ZWF1), glycolysis (PGI1) and TCA cycle (LPD1) in genotypes resulting from HG and LG trajectories. Each row represents the interactions associated to one genotype; in both cases the bottom row shows the epistasis in the WT for reference. It can be observed that the WT structure is conserved in a significant proportion of HG genotypes. In contrast, LG genotypes show a) less conservation of the WT pattern, b) generally more epistasis than in the WT, and c) a predominance of negative interactions, all of them patterns also significant at the statistical level (main text).

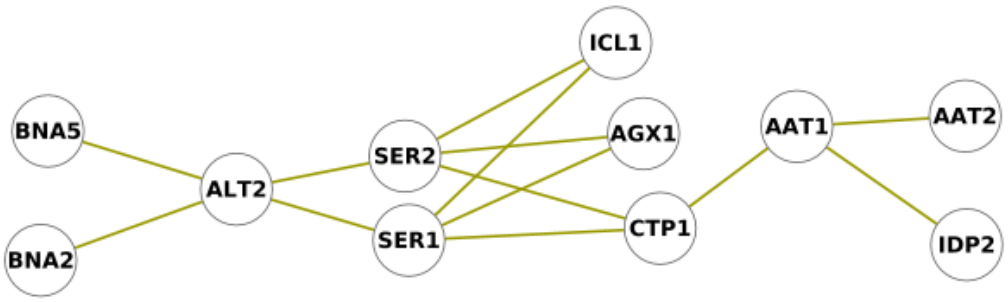

Figure S27. Synthetic lethal cluster 1.

Synthetic lethal interactions in *Saccharomyces cerevisiae* `iND750` model

We inspected in detail the mechanistic underpinnings of synthetic lethal (SL) interactions in the WT `iND750` metabolic model of *S. cerevisiae*. In contrast to the rest of interactions (which form a densely connected component), SL ones appear dispersed in several smaller network clusters that are mostly associated to biosynthetic functions.

Synthetic lethal cluster 1

We start with the biggest cluster shown in Fig. S27. The interactions that compose this cluster are specified in the following table,

Gene	Syst. name	Reactions coded
ALT2	YDR111C	Alanine transaminase
		α-ketoglutarate + Ala $\rightleftharpoons$ Glu + pyruvate
BNA2	YJR078W	Tryptophan 2,3-dioxygenase
		Trp + O_2 $\rightleftharpoons$ N-formyl-kynurenine
BNA5	YLR231C	Kynureninase
		kynurenine + H2O $\rightleftharpoons$ anthranilate + Ala
SER2	YGR208W	Phosphoserine phosphatase
		phosphoserine + H2O $\rightleftharpoons$ Ser + Pi
SER1	YOR184W3	Phosphoserine aminotransferase
		phosphoserine + α-ketoglutarate $\rightleftharpoons$ 3-phosphohydroxypyruvate + Glu
AGX1	YFL030W	Alanine:glyoxylate aminotransferase
		Ala + glyoxylate $\rightleftharpoons$ pyruvate + glycine
ICL1	YER065C	Isocitrate lyase
		isocitrate $\rightleftharpoons$ glyoxylate + succinate
CTP1	YBR291C	Mitochondrial inner membrane citrate transporter
		citrate[c] + malate[m] $\rightleftharpoons$ citrate[m] + malate[c]
AAT1	YKL106W	Mitochondrial aspartate aminotransferase
		α-ketoglutarate + Asp $\rightleftharpoons$ oxaloacetate + Glu
		Mitoch. erythrohydroxyglutamate α-ketoglutarate aminotransferase
		Mitoch. tyrosine aminotransferase
AAT2	YLR027C	Aspartate aminotransferase
		α-ketoglutarate + Asp $\rightleftharpoons$ oxaloacetate + Glu
		aspartate aminotranferase peroxisomal
		Erythrohydroxyglutamate α-ketoglutarate aminotransferase
		Perox. erythrohydroxyglutamate α-ketoglutarate aminotransferase
		tyrosine aminotranferase
		α-ketoglutarate + Asp $\rightleftharpoons$ oxaloacetate + Glu
		Perox. tyrosine aminotranferase
IDP2	YLR174W	Isocitrate dehydrogenase (NADP+)
		isocitrate + NADP+ $\rightleftharpoons$ α-ketoglutarate + CO2 + NADPH + H+

Here, the interactions between ALT2 and both BNA2 and BNA5 reflect alternatives for alanine biosynthesis. In WT conditions, alanine is synthesized by ALT2 from pyruvate and glutamate. In absence of ALT2, Alanine starts to be synthesized through the Trp degradation pathway via

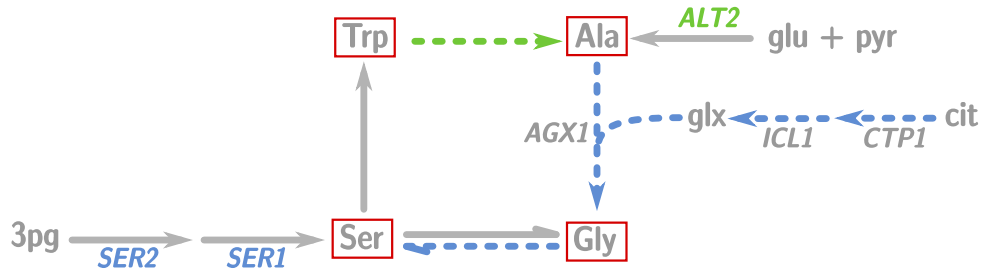

Figure S28. Alternative pathways for synthesis of Ala, Ser, Gly and Trp. Gray arrows indicate fluxes in the WT metabolism. Blue arrows indicate fluxes that appear when gene names colored in blue are deleted; analogously, green arrows are fluxes that activate upon deletion of the gene colored in green.

kynureine, for which both `BNA2` and `BNA5` are needed. In this path, Ala is synthesized with anthranilate as a byproduct of the kynureinase reaction. Anthranilate returns again to Trp production; and Trp reenters the cycle to continue producing Ala. The excess of Trp needed to compensate its outflow to Ala is supplied by higher flux in Trp synthesis from chorismate, see pathways in the following web links:

tryptophan degradation via kynurenine

tryptophan biosynthesis

superpathway of phenylalanine, tyrosine and tryptophan biosynthesis

Moreover, the interactions between `SER1` and `SER2`, and `CTP1`, `ICL1` and `AGX1` reflect alternatives for Ser and Gly production (as the latter is produced from Ser). In the WT, Ser is produced from glycolytic 3-phosphoglycerate by `SER1` and `SER2`. In absence of any of these genes, Gly starts being synthesized from glyoxilate (for which `CTP1`, `ICL1` and `AGX1` are required) and Ala. These metabolic changes are delineated in Fig. S28.

Fig. S28 further shows that, if both `ALT2` and one of `SER2` and `SER1` are lacking, Ala is needed to obtain Gly, Ser and Trp, but Ser and Trp are needed for Ala, originating the SL interactions among these three genes. Indeed, we were able to recover growth in these double mutants when supplemented with one of Ala, Gly or Ser. Supply of Trp on the contrary did not recover growth because Ser is synthesized from Trp but is in turn needed to refill the Trp degradation cycle through kynureine.

In this first SL cluster (Fig. S27), we identify as well interactions between AAT1, AAT2, CTP1 and IDP2. The Aspartate aminotransferases AAT2 (cytosolic) and AAT1 (mitochondrial) constitute in this model the only alternatives for Asp biosynthesis. But some additional metabolic readjustments occur upon removal of AAT1. Firstly, Glu produced in mitochondria from α-ketoglutarate has to be imported from the cytosol in order to synthesize 2-oxoadipate, in the Lys synthesis pathway. As the system starts to consume more Glu than synthesized, this becomes restored through export of mitochondrial citrate to cytosol (by CTP1), and transformation to α-ketoglutarate (by IDP2; α-ketoglutarate is converted in turn to Glu). This underlies the SL interactions of AAT1 with CTP1 and IDP2. Indeed, in the CTP1-AAT1 or IDP2-AAT1 double deletion, growth can be recovered by adding either Glu or α-ketoglutarate. Moreover, if the GDH3 gene (α-ketoglutarate to Glu) is removed, α-ketoglutarate stops being able to recover growth in this double deletion, showing that its supply is used for replacing Glu.

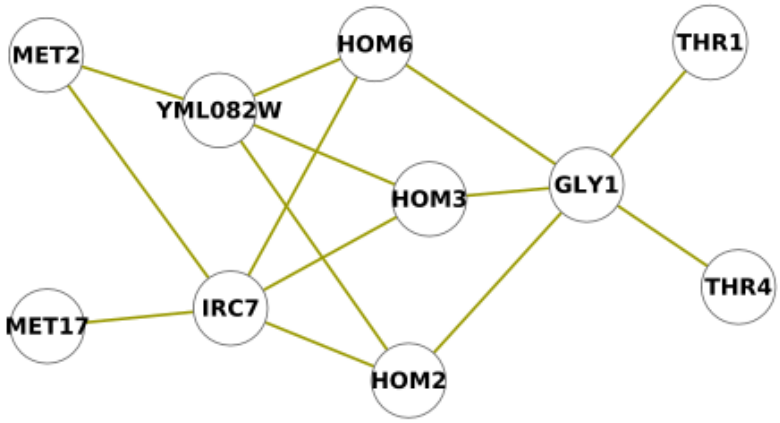

Figure S29. Synthetic lethal cluster 2.

Synthetic lethal cluster 2

In the second cluster (Fig. S29), SL interactions with `GLY1` denote different alternatives for Thr biosynthesis. In the WT, Thr is synthesized from Gly and acetaldehyde by `GLY1`. Alternatively, Thr can be also obtained from homoserine through `THR1` and `THR4`. In turn, `HOM2`, `HOM3` and `HOM6` are needed for biosynthesis of homoserine from Asp, and this is the rationale of the interactions of these genes with `GLY1`.

Interactions in the left of Fig. S29 are linked to homocysteine biosynthesis (needed for Met and phosphatidilcholine). In the pathway used in the WT, Thr is transformed to 2-oxobutanoate (in the Thr deaminase reaction, coded by two redundant genes); 2-oxobutanoate is then transformed into cystathionine by `YML082W` (and succinylhomoserine lyase, a gene-orphan reaction in the model). Finally, cystathionine is transformed into homocysteine by `IRC7`. In the alternative pathway, homocysteine is synthesized from Asp via homoserine in a pathway involving `HOM3`, `HOM2`, `HOM6`, `MET2` and `MET17`. These being the two alternatives for Met biosynthesis; thus, genes in one pathway interact negatively with genes in the other.

Gene	Syst. name	Reactions coded
GLY1	YEL046C	Threonine aldolase
		Thr ⇌ Gly + acetaldehyde
THR4	YCR053W	Threonine synthase
		phosphohomoserine + H2O ⇌ Thr + Pi
THR1	YHR025W	Homoserine kinase
		homoserine + ATP ⇌ phosphohomoserine + ADP + 2H+
HOM2	YDR158W	Aspartic beta semi-aldehyde dehydrogenase
		Aspartate semialdehyde + NADP+ + Pi ⇌ phosphoaspartate + H+ + NADPH
HOM3	YER052C	homoserine kinase activity
		homoserine + ATP ⇌ phosphohomoserine + ADP + 2 H(+)
HOM6	YJR139C	homoserine dehydrogenase
		homoserine + NADP+ ⇌ aspartate semialdehyde + NADPH + H+
IRC7	YFR055W	cystathionine beta-lyase
		cystathionine + H2O ⇌ homocysteine + NH3 + pyruvate
YML082W	YML082W	-
		succinylhomoserine + H2O ⇌ 2-oxobutanoate + succinate + NH4 + H+
MET2	YNL277W	homoserine O-transacetylase
		homoserine + acetyl-CoA ⇌ Acetylhomoserine + CoA
MET17	YLR303W	O-acetylhomoserine (thiol)-lyase
		Acetylhomoserine + H2S ⇌ homocysteine + acetate

An additional question is why, while MET2 interacts with both YML082W and IRC7, MET17 interacts only with IRC7. The explanation is that cystathionine can be alternatively synthesized from acetylhomoserine and Cys by STR2 (which is a slightly more inefficient mechanism). See also the web links below

superpathway of threonine and methionine biosynthesis

threonine degradation

superpathway of methionine biosynthesis

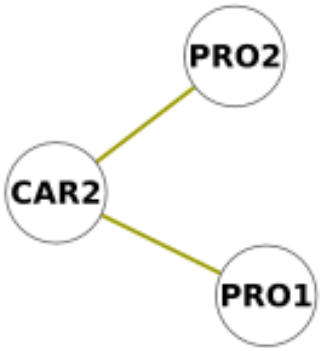

Figure S30. Synthetic lethal cluster 3.

Synthetic lethal cluster 3

Gene	Syst. name	Reactions coded
PRO1	YDR300C	Gamma-glutamyl kinase
		Glu + ATP ⇌ glutamyl-5-phosphate + ADP + H+
CAR2	YLR438W	L-ornithine transaminase
		ornithine + a 2-oxoacetate ⇌ glutamate semialdehyde + Glu
PRO2	YOR323C	Gamma-glutamyl phosphate reductase
		glutamate-5-semialdehide + NADP+ + Pi ⇌ glutamyl-5-phosphate + H+ + NADPH

In WT conditions, Pro is synthesized from Glu in a linear pathway that sequentially involves PRO1 and PRO2 whose result is glutamate-5-semialdehyde. When one of these genes is mutated, an alternative for Proline biosynthesis is to use CAR2 in the Arg degradation pathway. See also web links below

arginine degradation

proline biosynthesis

Figure S31. Synthetic lethal cluster 4.

Synthetic lethal cluster 4

Gene	Syst. name	Reactions coded
PSD2	YGR170W	phosphatidylserine decarboxylase, golgi and vacuole
		phosphatidylserine + H+ ⇌ phosphatidylethanolamine + CO2
PSD1	YNL169C	Phosphatidylserine decarboxylase, mitochondria
		phosphatidylserine + H+ ⇌ phosphatidylethanolamine + CO2
ATH1	YPR026W	acid trehalase (vacuole)
		trehalose + H2O ⇌ 2 glucose

In WT conditions, phosphatidilserine is synthesized in mitochondria by PSD1. An alternative mechanism is its synthesis in vacuole by PSD2. For this, however, trehalase has to be imported to vacuole and degradated to glucose, supplying the vacuolar proton needed for PSD2. Therefore, both enzymes are SL with PSD1.

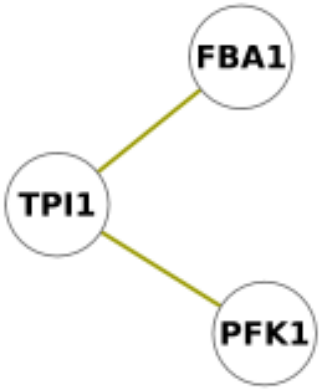

Figure S32. Synthetic lethal cluster 5.

Synthetic lethal cluster 5

Gene	Syst. name	Reactions coded
TPI1	YDR050C	triose-phosphate isomerase
		glyceraldehyde-3-phosphate ⇌ glycerone phosphate
PFK1	YGR240C	phosphofructokinase
		ATP + fructose-6-phosphate ⇌ ADP + fructose-1,6-bisphosphate
FBP1	YKL060C	Fructose 1,6-bisphosphate aldolase
		fructose-1,6-bisphosphate ⇌ DHAP + glyceraldehyde-3-phosphate.

Apparently, these enzymes should not interact negatively, as they perform their function sequentially in glycolysis. However, they present an additional function necessary for growth, the generation of DHAP in a small, but essential, quantity that is required for phospholipid biosynthesis. DHAP can only be generated by TPI1 from glyceraldehide-3-phosphate, or by FBP1 from fructose-1,6-bisphosphate which is in turn produced by PFK1. Thus, although most of the DHAP from the fructose bisphosphatase reaction is transformed to glyceraldehyde-3-phosphate for glycolytic progression, a very small quantity of DHAP is essential for biosynthetic causes.

Figure S33. Synthetic lethal cluster 6.

Synthetic lethal cluster 6

Gene	Syst. name	Reactions coded
ALD6	YPL061W	aldehyde dehydrogenase
		acetaldehyde + NADP+ + H2O ⇌ acetate + NADPH + H+
ALD4	YOR374W	Mitochondrial aldehyde dehydrogenase
		acetaldehyde + NADP+ + H2O ⇌ acetate + NADPH + H+
ADH3	YMR083W	Mitochondrial alcohol dehydrogenase
		ethanol + NAD+ ⇌ acetaldehyde + NADH + H+

These interactions reflect the two alternatives (cytosolic and mitochondrial) to obtain acetate, which is in turn needed to produce acetyl-CoA.

Rest of synthetic lethal interactions (isolated pairs)

MET22 - PMP1

Gene	Syst. name	Reactions coded
PMP1	YCR024C-A	ATPase cytosolic
		ATP + H2O → ADP + Pi + H+
MET22	YOL064C	3,5-bisphosphate nucleotidase
		adenosine-3',5'-bisphosphate + H2O ⇌ adenosine 5'-phosphate + Pi

PMP1 codes in the model for ATP hydrolysis to produce ADP, important for adjusting the ATP

$\rightleftharpoons$ ADP homeostasis. As an alternative, adenosine-5-phopsphosulfate is transformed to AMP by MET22, that combines later with ATP to produce 2ADP by adenilate kinase (a flux that also increases considerably in ΔPMP1). This alternative pathway to ADP homeostasis maintenance consumes 2 extra ATP molecules, which is the explanation of the fitness decrease on ΔPMP1.

APA1 - MET3

Two ways for the first step of SO4 fixation to produce adenosine-5-phopsphosulfate. Through APA1 –used in WT conditions– it is fixed over ADP; through MET3, it is fixed over ATP and produces pirophosphate that is an energetically more costly alternative.

ACO2 - ACO1

Mitochondrial aconitase redundancy. Additionally, ACO1 also performs cytosolic aconitase, which is the reason of keeping both genes in the dataset (see Materials and Methods, main text).

ACH1 - ACS2

Two different ways to synthesize acetyl-CoA from acetate. One of them involves ATP hydrolysis to AMP and PPi (ACS2), and the other does not (ACH1) and is the alternative used by the WT. The energetic difference is responsible for a lower fitness of ΔACH1

LEU4 - LEU9

2 isopropylmalate synthase redundancy. Additionally, LEU4 can also perform this activity in mitochondria, this difference being responsible for keeping both in the dataset.

TPS3 - TSL1

These two genes both code for two reactions, trehalose phosphatase and alpha-trehalose phosphate synthase. They are maintained in the dataset because of a different role in these reactions: while TSL1 is an essential sububnit, TPS3 is interchangeable (by TPS2, which is not kept in the dataset).

ARO3 - ARO4

Both genes code for 3-deoxyarabinoheptulosonate-7-phosphate synthetase. However, ARO3 codes additionally for the mitochondrial version of the reaction.

Synthetic lethal interactions: concluding remarks.

Synthetic lethal interactions were analyzed in this supplementary section in order to better understand their mechanistic underpinnings. Generally, most SL interactions arise from either paralell pathways or redundant genes. Some more intrincate architectures (such as the one associated to synthesis of Ala, Trp, Ser and Gly, see Figs. S27- S28) were also found. In that particular case, a set of inter-conversions between several essential biomass constituents led to a relatively big cluster of SL interactions.

It is also important to emphasize that SL interactions are systematically associated to biosynthetic functions. This is not observed only for genes that clearly belong to biosynthetic pathways. For instance, although TPI1, PFK1 and FBA1 (Fig. S32) are clearly catabolic genes, the SL interactions between them reflect an important biosynthetic function that is linked to providing DHAP for phospholipid biosynthesis. Moreover, these genes also display other types of interactions (e.g., weak negative or positive) which are clearly related to their catabolic activity. This further stresses the functional segregation of SL and the rest of epistatic interactions in biosynthetic and catabolic functions, respectively.

References

1. P Dürre and JR Andreesen, Journal of General Microbiology, **128**, 7, 1457–1466 (1982)

2. Y Benjamini and D Yekutieli, Annals of Statistics **29**, 4, 1165-1188 (2001)

3. B Szappanos *et al*, Nature Genetics, **43**, 7, 656–662 (2011)